

BIROn - Birkbeck Institutional Research Online

Gouw-Bouman, M. and van Asch, N. and Engels, Stefan and Hoek, W. (2019) Late Holocene ecological shifts and chironomid-inferred summer temperature changes reconstructed from lake Uddelermeer, the Netherlands. *Palaeogeography, Palaeoclimatology, Palaeoecology* , ISSN 0031-0182. (In Press)

Downloaded from: <https://eprints.bbk.ac.uk/id/eprint/28866/>

Usage Guidelines:

Please refer to usage guidelines at <https://eprints.bbk.ac.uk/policies.html>

or alternatively

contact lib-eprints@bbk.ac.uk.

Late Holocene ecological shifts and chironomid-inferred summer temperature changes reconstructed from Lake Uddelermeer, the Netherlands

M.T.I.J. Gouw-Bouman^a, N. van Asch^b, S. Engels^c, W.Z. Hoek^a

^a Utrecht University, Faculty of Geosciences, Dept. of Physical Geography, Princetonlaan 8A, 3584 CB, Utrecht, The Netherlands

^b ADC Archeoprojecten, Nijverheidweg-Noord 114, 3812 PN Amersfoort, the Netherlands

^c Birkbeck University of London, Department of Geography, 32 Tavistock Square, WC1H 9EZ, London, United Kingdom

*Corresponding author e-mail: mtij.gouw@gmail.com

Abstract

This paper presents a Late-Holocene chironomid-inferred July-air temperature record from a core obtained from Lake Uddelermeer in the Netherlands. A core interval, which dates from 2500 to 400 cal. yr. BP, was analysed at multi-decadal resolution for organic content, pollen, spores and NPPs (Non Pollen Palynomorphs), and chironomid head capsules. These proxies indicate that, from 2500 to 1140 cal. yr. BP, the lake was mesotrophic and sustained a *Littorellion*, while the chironomid assemblage was dominated by littoral species associated with macrophytes. At 1140 cal. yr. BP a shift in the lake ecology occurred from low-nutrient to high-nutrient conditions dominated by algae. This shift might be linked to a concurrent increase in human impact and is reflected in the chironomid assemblage by increases in eurytopic taxa, which are resistant to disturbances. Shifts in the chironomid record between 2500 and 1140 cal. yr. BP do not coincide with changes in lake ecology and are presumably driven by climate change. Using a Norwegian-Swiss calibration dataset as a modern analogue, we produced a chironomid-inferred temperature (C-IT) reconstruction. This reconstruction compares well to other regional temperature reconstructions in timing and duration with a Roman Warm period between 2240-1760 cal. yr. BP, a Dark Age Cold Period starting at 1760 cal. yr. BP and the Medieval Climate Anomaly beginning at 1280 cal. yr. BP. The C-IT record indicates a temperature drop of 1.5°C from the Roman Warm Period to the Dark Age Cold Period. Findings improve knowledge of the first millennium AD in NW Europe, which was characterised by changes in landscape, vegetation, society and climate.

Keywords

first millennium AD; non-biting midges; July air temperature; Dark Age Cold Period; Roman Warm Period; North-western Europe

1 Introduction

Many studies have shown that past climate fluctuations might be temporally linked to cultural shifts (Tinner *et al.* 2003; Büntgen *et al.* 2011; McCormick *et al.* 2012a; Büntgen *et al.* 2016). During the first millennium AD two large cultural transitions occurred in NW Europe: the decline of the Roman Empire and the later transition to medieval kingdoms. Recent studies (e.g. Büntgen *et al.* 2016b; Helama *et al.* 2017a; Helama *et al.* 2017b) have shown that climate in NW Europe during the first millennium was not as stable as previously assumed or as

41 evidenced from global climate reconstructions (Rasmussen *et al.* 2006; Vinther *et al.* 2006; Wanner *et al.* 2008).
42 Riechelmann and Gouw-Bouman (2019) indicate the presence of a Roman Warm Period (RWP; 1950-1700 cal.
43 yr. BP), a Dark Age Cold Period (DACP; 1700-1250 cal. yr. BP) and a Medieval Warm Period or Medieval Climate
44 Optimum (MCA; 1250-950 cal. yr. BP) in NW Europe (table 1). Other climate reconstructions from the Northern
45 Hemisphere also demonstrate the occurrence of significant climatic shifts during this time interval (e.g. Larsen *et al.*
46 *et al.* 2008; Ljungqvist 2010; Wanner *et al.* 2011; Gräslund and Price 2012; McCormick *et al.* 2012b; Büntgen *et al.*
47 2016b; Toohey *et al.* 2016; Helama *et al.* 2017a). The identification of similar warm and cold periods in numerous
48 proxy records throughout NW Europe indicates a regional climate trend (Helama *et al.* 2017a; Riechelmann and
49 Gouw-Bouman 2019).

50 Following the collapse of the Roman Empire a decrease in population density, from approximately 1680-
51 1450 cal. yr. BP (AD 270 to AD 500), was seen in the Netherlands, this time period is also known as the Migration
52 Period. This was followed by an exponential population growth from 1350 cal. yr. BP (AD 600) onward when the
53 medieval kingdoms emerged (Pierik and van Lanen 2017; Groenewoudt and van Lanen 2018; Pierik *et al.* 2018)
54 (table 1). Not only do these cultural shifts occur contemporaneously with climatic changes, they also are
55 concurrent with large-scale landscape and vegetation changes in the Netherlands (Jansma *et al.* 2014; Pierik
56 2017). In the Rhine-Meuse delta flooding frequency and intensity increased between 1700 cal. yr. BP and 1100
57 cal. yr. BP and multiple avulsions are placed within this time frame (Stouthamer and Berendsen 2000; Erkens
58 2009; Toonen 2013; Cohen *et al.* 2016; Pierik *et al.* 2017). In the Dutch coastal area increased storm surges are
59 observed from 1350 cal. yr. BP onward (Knol 1993; Vos and Van Heeringen 1997; Pierik *et al.* 2016).
60 Contrastingly, a decrease in aeolian activity is visible during the Roman period (1950-1550 cal. yr. BP) in the
61 Pleistocene cover-sand areas and an increase in driftsand activity took place at the end of the first millennium
62 around 1050 cal. yr. BP (Pierik *et al.* 2018). Vegetation development during the first millennium AD is
63 characterised by a reforestation phase between 1850 cal. yr. BP and 1250 cal. yr. BP. Although timing and
64 magnitude vary, this reforestation trend is recognised at most palynological study sites in the Netherlands and
65 neighbouring Germany (e.g. Teunissen 1990; Bunnik 1999; Kalis *et al.* 2008; Litt *et al.* 2009; Dörfler *et al.* 2012).

66 Although all climate, landscape, vegetation and population changes during the first millennium AD are
67 concurrent and some relation among them seems indisputable, the exact influence of each of these factors
68 remains unknown. It is therefore essential to obtain detailed and well-dated evidence of these changes to
69 disentangle the cause and effect of human impact, climate, landscape and vegetation change during the first
70 millennium AD.

71 Yet, detailed climate data from the Netherlands for the first millennium AD are at present not available.
72 This is probably due to the scarcity of archives suitable to study for this important time interval. Pristine natural
73 archives such as peat bogs and lake fills are often no longer present due to peat excavation, artificial drainage
74 and other human disturbances. Lake Uddelermeer, located in a cover-sand area in the central part of the
75 Netherlands, is a unique site as it contains an undisturbed sediment profile covering the last ca. 14,000 years
76 (Engels *et al.* 2016).

77 Chironomids, or non-biting midges, are an excellent proxy for the reconstruction of past summer
78 temperatures because they have a short life cycle and are sensitive to changes in temperature (Brooks *et al.*
79 2007; Telford and Birks 2011; van Asch 2012; Heiri *et al.* 2014). They have mainly been used to study Lateglacial
80 temperature variability but have been proven to be good proxy for Holocene temperatures as well (Axford *et al.*
81 2009; Millet *et al.* 2009; Brooks *et al.* 2012; Nazarova *et al.* 2013). However, as a result of human interference in
82 the environment, chironomid-inferred temperature reconstructions for the Late Holocene can be problematic.
83 Even small-scale human impact such as Prehistoric farming has been shown to impact chironomid communities
84 and distort the climate signal (Taylor *et al.* 2013; Taylor *et al.* 2017a; Taylor *et al.* 2017b). Therefore, a multi proxy
85 approach is recommended as a method for Holocene climate reconstructions, to infer possible human impact on

86 the record, and to disentangle the effects of natural processes such as climate change from anthropogenic
87 impacts on the landscape (McKeown and Potito 2016; Taylor *et al.* 2018).

88 The aims of this study are fourfold: (1) to present the first chironomid record from the Netherlands
89 covering the first millennium AD on a multi-decadal scale, (2) to determine, using the sedimentological,
90 palynological and chironomid records, to what extent human impact influenced the lake ecology and whether
91 temperature is the main environmental driver of changes in the chironomid assemblage, (3) to assess whether
92 absolute chironomid-inferred summer-temperature values are realistic and, (4) to assess whether the chironomid-
93 inferred temperature reconstruction shows evidence for temperature change during known phases of changing
94 climate.

95

96 **2 Area description**

97 Lake Uddelermeer is a pingo remnant located on the Veluwe (52°14'48"N; 5°45'40"E; 24-27 m a.s.l.)
98 (Fig. 1). The pingo remnant is situated at the head of a periglacial valley, in the cover-sand area between the ice
99 pushed ridges of Ermelo (max. elevation ca. 50 m a.s.l.) and Apeldoorn (max. elevation ca. 100 m a.s.l.) (Fig. 1)
100 and in the subsurface an impermeable clay layer is present. These boundary conditions are typical for the
101 occurrence of pingos in the Netherlands due to the presence of a ground water gradient and/or pressure. This is
102 evidenced by the presence of another pingo remnant in this area: Lake Bleekemeer, which does not contain a
103 complete Late Holocene lake infill due to peat cutting (Polak 1959).

104 Lake Uddelermeer is oval shaped, 200-300 metres in diameter and has a current maximum water depth of 1.3
105 metres (Engels *et al.* 2016). The total lake sediment infill reaches a maximum depth of 15.6 metres of which 12.9
106 metres covers the Holocene. The lake is fed by groundwater and a small brook is draining the south-side of the
107 lake (Staverdense or Leuvenumse beek). The area directly surrounding the lake is slightly elevated, limiting inflow
108 of surface water runoff into the lake (Fig. 1). The lake is currently eutrophic and directly surrounding the lake is an
109 alder carr and a fringe of wetlands with reeds. The regional vegetation consists mainly of mixed oak and birch
110 forest, grasslands and agricultural fields. Average July temperature for the period 1901-2017 in de Bilt (ca. 50 km
111 SW of Lake Uddelermeer) is 16.95 °C (1901-1950 = 16.4 °C) (Royal Netherlands Meteorological Institute;
112 www.knmi.nl)

113 Archaeological finds in the vicinity of the lake indicate the presence of human activities from the Middle
114 Mesolithic onward (Groenewoudt *et al.* 2006). Neolithic (7250-3950 cal. yr. BP; 5300-2000 BC) burial mounds
115 from the Trechterbeker culture (5350-4850 cal. yr. BP; 3400-2900 BC) are present at a distance of ca. 500 metres
116 from the lake. There is also evidence of charcoal production in the direct surroundings of the lake during the 9th
117 and 10th centuries (Kraanen and Pape 1965). Situated next to the lake is a medieval structure dating to the late
118 10th century (Heidinga 1987). This so-called Huneschans is a medieval ring fort (*ringwalburg*) which is
119 approximately 100 metres in diameter, and is surrounded by a circular earthen wall and an outer ditch. The
120 earthen wall is not fully circular, with an opening present on the side of the lake. The wall currently does not reach
121 the lake itself, indicating that the water level of the lake was up to 1.7 metres higher during the time of
122 construction of the fort (10th century; Engels *et al.* 2016). Earlier palynological studies by Engels *et al.* (2016),
123 Bohncke (1999), Sohl (1983) and Polak (1959) show the first evidence of human activities at the beginning of the
124 Subboreal at 5000 cal. yr. BP, which is concurrent with the construction of the burial mounds encountered in the
125 area (Groenewoudt *et al.* 2006). Pollen records covering this period show an increase of *Corylus* and *Pteridium*
126 indicating open forests as well as the occurrence of human indicators such as *Plantago* and *Cerealia*. From 4000
127 cal. yr. BP onward the human-induced deforestation trend, which initiated around 5000 cal. yr. BP, increased.

128 Human presence in the form of agriculture is continuous from 3450 cal. yr. BP onwards as indicated by a
129 continuous *Cerealia* pollen curve (Engels *et al.* 2016).

130

131 *Figure 1 around here*

132

133 **3 Methods**

134 A 16-metre-long sediment core (\varnothing 6 cm) was collected from the deepest part of the lake in April-May
135 2012 using a piston corer operated from an UWITEC coring platform. The lake infill was cored in 3 metre sections
136 using overlapping cores, and coring tubes were subsequently cut to 1 metre intervals in the field to enable
137 transport. In the lab the core segments were cut in half lengthwise, where one part was completely preserved and
138 the other half was used for sampling. A continuous 1 cm sampling was carried out for Loss on Ignition (LOI) to
139 determine organic content following the protocol by Heiri *et al.* (2001). A total of 437 samples of ca. 1 cm³ were
140 dried at 105° C for 12 hours and subsequently placed in an oven at 550° for 4 hours. The samples were weighed
141 before and after each step, obtaining both the moisture as well as the organic carbon content. Pollen samples of
142 0.7 cm³ were collected using a 5 cm sampling resolution for the section 100-500 cm below the sediment/water
143 interface to obtain a high-resolution vegetation record capable of detecting the fast vegetation changes during the
144 first millennium AD in detail. In total 70 pollen samples were prepared following the method described in Faegri
145 and Iversen (1989) and Moore *et al.* (1991). Identification of pollen, spores and Non Pollen Palynomorphs (NPPs)
146 was executed using a Zeiss microscope with 400x magnification and pollen and spores were identified using
147 Beug (2004), Moore *et al.* (1991) and Punt (1976; 1980; 1981; 1984; 1988; 1991; 1995; 2003). NPPs such as
148 algal remains and (fungal) spores were identified using van Geel *et al.* (2003), van Geel (1978) and van Geel
149 (1972). An upland pollen sum of 300 pollen grains, excluding alder and grasses, was counted per sample. This
150 pollen sum differs from the one used in Engels *et al.* (2016), as grasses and alder pollen are excluded from the
151 pollen sum in this study since reed land (included in the Poaceae curve) and alder carr occur locally.

152 The sediment record was previously analysed for chironomids at a coarse temporal resolution by Engels
153 *et al.* (2016). For the current research, additional chironomid samples were analysed to increase the temporal
154 resolution from the section 200-500 cm below the sediment surface to detect the short climatic phases during the
155 first millennium AD. From this section, a total of 31 samples were analysed at 5-25 cm resolution. In order to get a
156 better overview of preceding and subsequent trends, the lower temporal resolution results from Engels *et al.*
157 (2016) from the sections 100-200 cm and 500-550 cm are also included in this study. Sample preparation for
158 these samples is described in Engels *et al.* (2016). The additional samples (14 in total, sample size: 0.335 cm³)
159 were added to a 5% KOH solution, heated to 90°C for 1 hour, and then passed successively through 212 μ m and
160 90 μ m mesh sieves. Chironomid head capsules were manually picked out of the sieving residues using a Bogorov
161 sorting tray under a dissection microscope (40x magnification) and subsequently mounted on permanent slides in
162 Euparal®. Chironomid head capsules were identified under a compound microscope (magnification 400x)
163 following keys by Wiederholm (1983), Moller Pillot (1984a); Moller Pillot (1984b), Rieradevall and Brooks (2001)
164 and Brooks *et al.* (2007). Information on chironomid ecology was derived from a.o: Moller Pillot and Buskens
165 (1990), Brooks *et al.* (2007), Moller Pillot and Klink (2009), Engels and Cwynar (2011), Luoto (2011), Engels *et al.*
166 (2012), Moller Pillot (2013) and Potito *et al.* (2014). The number of identified chironomid head capsules varied
167 between 65 and 146 per sample. A Principal Component Analysis (PCA) with Square-root-transformed
168 percentage-abundance data of the chironomid taxa was executed using the program C2 (Juggins, 2003).

169 The chironomid assemblages were subsequently used to quantitatively reconstruct mean July air
170 temperatures. This reconstruction was executed using a chironomid-temperature inference model, which is based
171 on a modern calibration dataset that consists of 274 lakes from Norway and the Alpine regions (Heiri *et al.* 2011).

172 This chironomid-climate calibration dataset spans a July air temperature range from 3.5 to 18.4°C (Heiri *et al.*
173 2011). For the model, a two component weighted averaging partial least-squares (WA-PLS) regression was used
174 since this approach produced inference models with the lowest error (Heiri *et al.* 2011). The selected model had a
175 bootstrapped root mean square error of prediction of 1.40°C after outlier deletion (Heiri *et al.* 2011). Bootstrapping
176 was used to estimate the sample-specific errors for the fossil samples.

177 We evaluated the robustness of the chironomid-inferred July air temperature reconstruction by
178 calculating the closest modern analogue of the fossil samples, as well as the goodness-of-fit to temperature (Birks
179 *et al.* 1990) and the cumulative percentage of rare or absent species from the calibration dataset. The closest
180 modern analogue was assessed based on squared Chi-squared distances using the program C2 (Juggins, 2003).
181 Fossil samples with a distance to the closest analogue larger than the 2nd and 5th percentile of the distances of the
182 modern samples in the calibration dataset were classified as having 'no close' and 'no good' analogue,
183 respectively. Goodness-of-fit to temperature was assessed using a Canonical Correspondence Analysis (CCA) of
184 the modern samples with temperature as the only constraining variable. In this analysis, the fossil samples were
185 added passively. Fossil samples with a residual distance exceeding the 90th and 95th percentiles of the residual
186 distances of the modern samples were identified as having a 'poor' and 'very' poor fit with temperature,
187 respectively. The CCA was calculated using CANOCO for Windows version 4.51 (ter Braak and Šmilauer 2012).
188 Both the pollen percentage diagram as well as the chironomid abundance diagram were produced using TILIA
189 (Grimm 1991-2015). Zonation of the pollen and chironomid diagrams differs from Engels *et al.* (2016) as a result
190 of the increased sampling resolution in this study and was established visually. The pollen diagram was
191 subdivided into zones based on variations in the main pollen taxa and zonal boundaries were verified using
192 CONISS (Grimm 1991-2015). The chronology of the core is based on the age-depth model of Engels *et al.*
193 (2016), which is based on 26 samples for ²¹⁰Pb measurement for the top 65 cm of the core and 13 AMS
194 radiocarbon samples (excluding 3 outliers) throughout the rest of the core. The age-depth model was produced
195 using Bayesian modelling as included in Oxcal (Bronk Ramsey 2009). The radiocarbon samples contained
196 terrestrial macrofossils, wood fragments and charred material such as grass epidermis and charcoal (Engels *et al.*
197 2016). The age-depth chronology of the core section discussed in this paper (100 to 550 cm sediment depth) is
198 supported by six radiocarbon dates (excluding 1 outlier) and constrained at the top by the ²¹⁰Pb dates (Fig. 2).
199 The resultant age-depth model gives well-constrained age estimates and a nearly linear sedimentation rate,
200 confirming the reliability of the six dates included. All ages provided in this paper are rounded to the nearest five
201 year interval and are expressed in cal. yr. BP unless explicitly stated otherwise.

202
203 *Figure 2 around here*
204

205 **4 Results and interpretation**

206 **4.1 Sedimentology**

207 The investigated core interval consists entirely of gyttja (Fig. 3). The bottom part, 550 cm up to 220 cm
208 depth, consists of brown gyttja. From 220 cm upward this slowly shifts to a more greenish gyttja, indicating a
209 larger component of algae. The LOI-record follows this trend with values around 60% from 550 cm up to 460 cm
210 depth, followed by a more organic-rich sequence with values upward of 70%, until 270 cm depth. From 270 cm to
211 220 cm LOI values vary around 60% again and drop sharply to only 20% at 220 cm, which corresponds with the
212 shift to a higher algal content. The drop in organic content is probably the result of increased silica production
213 (a.o. diatom production) in the lake. Alternatively, an increase in sand input through increased aeolian activity
214 could explain this decrease. However, no visible sand grains were found during visual core inspection, suggesting

215 that an increase of silica production is the most likely reason for the observed decrease in LOI values. From 220
216 cm upwards, LOI values gradually increase, reaching 60% at 140 cm after which they gradually decrease to 30%.

217

218 *Figure 3 around here*

219

220 **4.2 Palynology**

221 Zone Pa (500-382 cm depth; 2420-1730 cal. yr. BP) is characterised by high values of Arboreal Pollen
222 (AP) and heather (Fig. 3). High values of deciduous tree species such as *Quercus*, *Fagus* and the occurrence of
223 *Carpinus*, *Tilia* and *Ulmus* suggest the presence of a mixed-deciduous forest in the vicinity of the lake. *Fraxinus*,
224 *Corylus* and *Betula* probably grew at the forest edge or in small bushes and thickets. Human presence in the area
225 around Lake Uddelermeer is indicated by high percentages of upland herbs with typical anthropogenic indicators
226 such as *Rumex*, *Plantago lanceolata* and *Artemisia vulgaris* and the presence of pollen grains of Cerealia,
227 indicating arable fields nearby. Heathlands are also present in the area, as evidenced from the large proportion of
228 *Calluna*. The lake was probably surrounded by an alder carr with grasslands in the vicinity and alder carr was
229 likely also present in the brook valley of the Leuvenumse beek to the south. The high values of both *Isoëtes* and
230 *Littorella* suggest relatively nutrient-poor and clear-water conditions in the lake itself. *Isoëtes* and *Littorella* are
231 both adapted to low nutrient conditions, by a symbiosis with mycorrhiza to enable carbon uptake from the
232 sediment, and a slow growth rate, and are therefore typical inhabitants of oligotrophic lakes, where they most
233 often grow in water of 0 to 2 metres deep (Sand-Jensen 1978; Weeda *et al.* 1988; Engels *et al.* 2018). *Isoëtes*
234 can grow in water up to 4.5 metres deep and prefers a sandy subsoil (Sand-Jensen 1978; Farmer and Spence
235 1986). Most likely *Littorella* also grew at the shore of the lake, since this species only flowers when it is not
236 submerged (Weeda *et al.* 1988). Together, both species form the *Littorellion* which is a relatively stress tolerant
237 plant community (Rørslett and Brettum 1989). However, when nutrient availability increases, macrophytes and
238 algae can more easily inhabit the lake. As a result *Littorella* and *Isoëtes* receive less light and the *Littorellion* is
239 fast replaced by reedlands (Weeda *et al.* 2000). The nutrient-poor conditions in the lake are confirmed by the
240 presence of *Nymphaea alba* which probably grew in the deeper parts of the lake. The algae *Botryococcus*, which
241 was present in Lake Uddelermeer continuously since the Late Glacial (Engels *et al.*, 2016), can occur in a wide
242 range of environments but has a preference for oligotrophic lakes (Padisák *et al.* 1998). Engels *et al.* (2016)
243 reconstructed a water depth of around 2.5-3 metres during this time period, which is in line with the 2 metres
244 suggested by the aquatic taxa present in the lake. Spores of *Glomus*, a fungus often found in soils, is present in
245 the upper part of this zone. The occurrence of *Glomus* spores in lake sediments is indicative of soil erosion (van
246 Geel *et al.* 2003).

247 Zone Pb (382-255 cm depth; 1730-1270 cal. yr. BP) is characterised by increasing values of AP and
248 decreasing values of heather and to a lesser extent upland herbs (Fig. 3). The increase in AP can be mainly
249 attributed to *Quercus*, *Fagus* and *Carpinus*. Anthropogenic indicators such as upland herbs (*Rumex*, *Plantago*
250 *lanceolata* and *Artemisia vulgaris*) and Cerealia decrease in this zone. Pollen grains of Cerealia are still present,
251 albeit in low abundances, and occasionally *Secale cereale* is found. These changes in the pollen assemblage
252 suggest that deciduous forests have expanded at the expense of heathlands and arable lands. We also observe
253 an increase of *Alnus* and a decrease of Poaceae suggesting that the local alder carrs are also expanding. The
254 basal cells of Nymphaeaceae (NPP type HdV-127) are decreasing sharply during this zone, although *Nymphaea*
255 *alba* is still present in the pollen record. *Nuphar lutea*, however, is nearly absent from zone Pb. The continued
256 presence of *Isoëtes* and *Littorella* suggests continued nutrient-poor and clear-water conditions in the lake. Pollen-
257 percentage values of *Littorella* however, are slightly decreasing. The occurrence of *Typha latifolia* pollen during
258 this zone indicates the presence of reed lands at the lake fringe which possibly partly replaced the *Littorellion*.

259 Zone Pc (255-220 cm depth; 1270-1140 cal. yr. BP) is a transitional zone which shows decreasing AP
260 values and increasing values of Cerealia and heather (Fig. 3). A mixed deciduous forest is still present but arable
261 lands and heathlands are fast expanding. This is also visible from the increase in anthropogenic indicators such
262 as Cerealia, *Plantago lanceolata*, a continuous curve of *Secale cereale* pollen, and an increase in the
263 occurrences of charcoal. The alder carr decreases in size and becomes more open with more grass or reed land,
264 as seen from the decreasing abundance of *Alnus* and increasing Poaceae values and the presence of *Typha*
265 *angustifolia*. *Isoëtes* and *Littorella* are still present in the pollen record indicating relatively stable conditions in the
266 lake through zone Pa, Pb and Pc. The water body must have remained clear enough throughout pollen zones Pa,
267 Pb and Pc to sustain the *Littorellion*.

268 Zone Pd (220-100 cm depth; 1140-320 cal. yr. BP) is characterised by further decreasing values of AP
269 and heather and increasing values of upland herbs and Cerealia (Fig. 3). The start of this zone is simultaneous
270 with the shift to green algal gyttja indicating a higher production in the lake. This is also evident from the rapidly
271 increasing values of algal remains such as *Scenedesmus* or *Pediastrum*. An increase in various algal species
272 from ca. 25% to over 100% occurs at 185 cm depth (1030 cal. yr. BP). In our record the abrupt increase in algal
273 remains coincides with increasing values of fungal spores of coprophilous fungi such as *Sporormiella*, *Podospora*
274 and *Cercophora* which are indicative for the presence of dung. The increase in algae also coincides with the
275 habitation phase of the Huneschans (late 10th cent.) and is most likely caused by increased nutrient input as a
276 result of human impact. Engels *et al.* (2018) however, found sediment age and water depth to be the most likely
277 explanatory variables for this ecosystem change. From 155 cm depth (1250-700 cal. yr. BP) onward *Cannabis*-
278 type shows an increase from ca. 1% to ca. 35% which is likely the result of the retting of hemp in the lake to
279 create hemp fibres for rope production. The practice of hemp retting in the Netherlands is known from the historic
280 record and also evidenced at Lake Uddelermeer from the high values of *Chaetomium* spores which are cellulose-
281 decomposers and occur among others, on decaying herbaceous stems (van Geel *et al.* 2003).
282 Overall zone Pd indicates an increase in human activity, with higher values of Cerealia, *Secale*, *Fagopyrum* and
283 *Sinapis*-type and various herbs such as *Rumex* and Amaranthaceae. The presence of charcoal also increases
284 during this zone, which might be linked to the charcoal production in the area. There are fewer deciduous tree
285 species present indicating the disappearance of the closed and mixed deciduous forest, which are being replaced
286 by more open oak forest with hazel and ash. Arable lands are expanding while the heathlands are decreasing.
287 The alder carr is also disappearing and is being replaced by grassland. In the lake itself the eutrophic conditions
288 are evident from the disappearance of *Littorella*, *Isoëtes* and *Nymphaea* and the concurrent increase of
289 *Myriophyllum alterniflorum*. The occurrence of this aquatic perennial is often linked to an increase in phosphate
290 (Roelofs *et al.* 1984). *Myriophyllum alterniflorum* grows in water up to 2 metres deep (Hannon and Gaillard 1997)
291 suggesting that water depth remained stable during the entire period, in line with results by Engels *et al.* (2016).

292
293 *Figure 4 around here*

294

295 **4.3 Chironomid record**

296 Chironomids are well preserved and abundant throughout the record. Our record has an average count
297 sum of 99 head capsules per sample (range 64-167). Most of the encountered chironomid taxa (e.g.
298 *Lauterborniella*, *Parakiefferiella bathophila*-type) are commonly found in the littoral zone of meso- to eutrophic
299 lakes and prefer warm or temperate conditions (Brooks *et al.* 2007, and references therein). Further, a number of
300 taxa present in the record are often associated with macrophytes (e.g. *Ablabesmyia*). The chironomid diagram is
301 divided into two zones Ch1 and Ch2, following major shifts in the chironomid assemblage, which correspond with
302 the major lithological units in the core (Fig. 4).

303 Chironomid zone Ch1 (550-220 cm; 2525-1140 cal. yr. BP) is dominated by *Lauterborniella*,
304 *Cladotanytarsus mancus*-type and *Parakiefferiella bathophila*-type which are all typical inhabitants of littoral zones
305 of lakes. In addition, *Lauterborniella* and *P. bathophila*-type are often associated with submerged vegetation
306 (Moller Pillot 1984b; Brooks *et al.* 2007; Moller Pillot and Klink 2009; Moller Pillot 2013). *Lauterborniella* is found in
307 the warmer lakes included in the Norwegian-Swiss calibration dataset (Heiri *et al.* 2011). Chironomid zone Ch1 is
308 further subdivided based on smaller changes in the abundance of the chironomid taxa.

309 Subzone Ch1a (550-470 cm depth; 2525-2240 cal. yr. BP) is marked by relatively high values of
310 *Endochironomus albipennis*-type and *Pseudochironomus* and the presence of *Limnophyes/Paralimnophyes* and
311 *Procladius*. Both *Pseudochironomus* and *E. albipennis*-type occur in the littoral of lakes (Brooks *et al.* 2007;
312 Engels *et al.* 2012). *E. albipennis*-type is often associated with macrophytes (Moller Pillot 1984b) suggesting the
313 presence of aquatic vegetation in the lake. This is in line with the pollen record, which indicates the presence of a
314 *Littorellion* and Nymphaeaceae. Based on the presence of *Littorella* and *Isoetes*, relatively nutrient-poor
315 conditions are expected in the lake. However chironomid taxa such as *P. bathophila*-type and *Polypedium*
316 *nubeculosum*-type are typically found in eutrophic lakes (Moller Pillot 2013). *Lauterborniella* is often ascribed to
317 eutrophic conditions (Moller Pillot 2013) but this genus has been found in oligotrophic lakes as well (Brodin 1986).
318 Based on the combination of the presence of aquatic macrophytes that typically occur in oligo- to mesotrophic
319 conditions and chironomid taxa that typically occur in meso- to eutrophic conditions we conclude that the lake was
320 probably mesotrophic throughout zone Ch1. This conclusion is further supported by the occurrence of taxa such
321 as *Pseudochironomus* and *Tanytarsus mendax*-type, which are inhabitants of mostly mesotrophic lakes (Moller
322 Pillot 2013). Further, *Limnophyes/Paralimnophyes*, *Lauterborniella*, *P. nubeculosum* and *Pseudochironomus* are
323 most often found in shallow lakes (Brooks *et al.* 2007; Engels *et al.* 2012), which is in line with the presence of the
324 *Littorellion* and the estimated water depth of 2.5 to 3 metres by Engels *et al.* (2016). *C. mancus*-type and *P.*
325 *bathophila*-type have a preference of lakes with a water depth less than 5 metres (Luoto 2011). The majority of
326 species present in this zone such as *E. albipennis*, *Procladius*, *C. mancus*-type are acidophilic which is also in line
327 with the reconstructed nutrient-poor, clear-water conditions in the lake. In the calibration dataset, *Procladius* and
328 *Limnophyes/Paralimnophyes* are both found along a large temperature gradient, including colder lakes, resulting
329 in relatively low temperature optima for these taxa (Heiri *et al.* 2011).

330 The onset of subzone CH1b (470-390 cm depth; 2240-1760 cal. yr. BP) is defined by the appearance of
331 *Parachironomus varus*-type and an increase of *Corynoneura edwardsi*-type and further characterized by the
332 absence of *Limnophyes/Paralimnophyes* and *Procladius*. *P. varus*-type and *C. edwardsi*-type are both often
333 associated with macrophytes and have relatively high temperature optima in the Norwegian-Alpine calibration
334 dataset (Heiri *et al.* 2011) (Brooks *et al.* 2007). At the start of this subzone, *E. albipennis*-type reaches maximum
335 values, directly followed by a strong decline from 19.2 % to 1.4%. *Lauterborniella* also reaches maximum values
336 in this subzone. *Pseudochironomus* is still present, although at slightly lower abundances than in the previous
337 subzone. *P. varus*-type is acidophobic (Brooks *et al.* 2007) suggesting less acidic conditions which is in line with
338 the drop in *Procladius* and *E. albipennis*-type which are both acidophilic. Nevertheless, other acidophilic species
339 such as *C. mancus*-type, *Psectrocladius sordidellus*-type are still present. We therefore conclude that the shift in
340 the chironomid fauna associated with the Ch1a/Ch1b-transition does not reflect any significant changes in the
341 lake ecosystem but rather a reorganization of the fauna already present in the lake.

342 Subzone Ch1c (390-255 cm depth; 1760-1270 cal. yr. BP) is defined by maximum values of *P.*
343 *bathophila*-type (35.7%) and is further marked by the reappearance of *Limnophyes/Paralimnophyes* and
344 *Procladius* and an increase in *P. sordidellus*-type and *P. nubeculosum*-type. *Lauterborniella* gradually declines
345 from its maximum abundance of 35.2% to values of 15.3% during subzone Ch1c. *Pseudochironomus* and *P.*
346 *varus*-type also reach lower abundances than in the previous subzone. Both *P. nubeculosum*-type and *P.*
347 *sordidellus*-type typically occur in the littoral zone of temperate lakes (Engels *et al.* 2012; Luoto 2012), although

348 according to Moller Pillot (1984b) *P. nubeculosum*-type is found in lakes with a depth up to 18 m. The increase in
349 *P. nubeculosum*-type, *P. bathophila*-type might suggest more nutrient-rich conditions in the lake. However,
350 oligotrophic and mesotrophic taxa such as *Heterotanytarsus* and *Pseudochironomus* are still present indicating
351 that conditions remained relatively nutrient poor.

352 The final subzone (Ch1d: 255-220 cm depth; 1270-1140 cal. yr. BP) is marked by higher values of *E.*
353 *albipennis*-type, while abundances of *Lauterborniella* and *P. bathophila*-type are lower than in the preceding
354 subzones. Taxa that appear or increase during this zone are *Glyptotendipes pallens*-type and *Polypedilum*
355 *sordens*-type which are both found in the warmer lakes in the training set. The most distinct feature of this
356 subzone, however, is the high abundance of *T. mendax*-type. This taxon consists of a large number of species
357 and is found in a range of environments (Brooks *et al.* 2007). The taxon also occurs along a wide temperature
358 range, but is absent from the coldest lakes (Heiri *et al.* 2011). *T. mendax*-type is sensitive to increases in
359 phosphate but can occur in all trophic states and prefers mesotrophic conditions. This species mostly lives in the
360 profundal zone and is most abundant in water over 5 metres deep. *E. albipennis*-type and *P. bathophila*-type have
361 similar nutrient preferences although *P. bathophila*-type is indicative for warmer conditions. The shifts that we
362 observe in the chironomid fauna during zone Ch1 do not coincide with shifts in ecology of the lake as
363 reconstructed from the pollen and LOI records. We therefore suggest that the changes observed in the
364 chironomid record were potentially driven by external factors such as climate change rather than by changes in
365 within-lake processes.

366 The onset of chironomid zone Ch2 coincides with the transition of brown gyttja to green algal gyttja (220-
367 100 cm depth; 1140-320 cal. yr. BP). Zone Ch2 is marked by increases or appearances of the chironomid taxa
368 *Microtendipes pedellus*-type, *Cladopelma lateralis*-type, *Cricotopus laricomalis*-type, *Nanocladius branchicolis*-
369 type and the Tanypodinae *Procladius* and *Ablabesmyia*. Zone Ch2 also shows an increase in the total number of
370 chironomid taxa found, with a maximum of 25 taxa at 149 cm. Of the dominant taxa in zone Ch1, *C. mancus*-type
371 and *P. bathophila*-type are still present in zone Ch2, while *Lauterborniella* strongly declines towards the upper
372 part of this zone. In addition, the chironomid assemblage still includes a.o. *E. albipennis*-type, *P. nubeculosum*-
373 type and *T. mendax*-type. Both the sedimentological and the palynological record indicate a strong shift in the
374 water quality of the lake during this time period, with more nutrient-rich and turbid conditions present after 1140
375 cal. yr. BP. This transition is reflected in the chironomid-species composition where most species with specific
376 habitat requirements such as the presence of aquatic macrophytes or low-nutrient levels decline in favour of
377 *Procladius* and *Ablabesmyia*. These latter two taxa are typically interpreted as generalists and are able to persist
378 in dynamic conditions (e.g. Vallenduuk and Moller Pillot 2007). *Ablabesmyia* prefers shallow, warm and still water
379 and is associated with macrophytes (Engels *et al.* 2012). Additionally, *Procladius* is sensitive to increases in
380 phosphate, can occur in acidified lakes and tolerates pollution well (Luoto 2011). *M. pedellus*-type is also often
381 encountered in dynamic environments and together with *Ablabesmyia* is found in shallow lakes of less than five
382 metres deep (Engels *et al.* 2008a; Engels *et al.* 2008b; Engels *et al.* 2012). Potito *et al.* (2014) found a relation
383 with high agricultural cover and the occurrence of this chironomid taxon, which is in line with the low AP values
384 and high upland herbs and Cerealia pollen percentages in this zone. *M. pedellus*-type however, has a preference
385 for mesotrophic conditions and a stable oxygen regime (Moller Pillot and Klink 2009), and Engels *et al.* (2018)
386 therefore suggested that this increase could be a relative increase, with other taxa decreasing faster under
387 unfavourable conditions than *M. pedellus*-type. Other taxa that indicate higher trophic conditions are e.g. *G.*
388 *pallens*-type, *Chironomus anthracinus*-type, *Chironomus plumosus*-type, *C. lateralis*-type, *Dicrotendipes*
389 *nervosus*-type. Overall, the combined proxy-records indicate a shift in the lake ecology from the clear-water
390 mesotrophic conditions of zone Ch1 to the eutrophic, turbid conditions of zone Ch2.

391
392 *Figure 5 around here*

394 4.4 Factors controlling the chironomid fauna composition of Lake Uddelermeer

395 The most important precondition to establish a C-IT reconstruction is that temperature fluctuations are
396 the main factor influencing the chironomid composition. This is especially important for Holocene temperature
397 reconstructions, since the amplitude of temperature fluctuations in e.g. the mid-latitudinal areas of the northern
398 Hemisphere, was small when compared to Late Glacial studies. Chironomid communities of shallow, temperate
399 lakes such as Lake Uddelermeer are especially sensitive to changes in the environment since dominant controls
400 on the chironomid composition like hypolimnetic oxygen depletion and climatic extremes are lacking (Langdon *et al.* 2006). Based on the sedimentological, palynological and chironomid record, conditions in the lake itself
401 remained stable with clear-water, nutrient-poor conditions during the interval between 2500 and 1140 cal. yr. BP
402 i.e. covering chironomid zone Ch1 and the pollen zones Pa, Pb and Pc. The strong eutrophication of the lake at
403 the onset of chironomid zone Ch2 is visible in the sediment core as a colour change, in the pollen record (here
404 zone Pd) as an increase in algal species, and in the chironomid record as an increase of generalists such as
405 *Ablabesmyia* and *Procladius* (Fig. 5). Together these changes indicate a significant ecosystem shift in Lake
406 Uddelermeer from mesotrophic clear-water conditions to more nutrient-rich and turbid conditions. This conclusion
407 is in line with results by Engels *et al.* (2018), who reconstructed stable clear-water conditions in Lake
408 Uddelermeer from 6000 cal. yr. BP onward and an increase in nutrient availability at 1030 cal. yr. BP from
409 sedimentary pigments, chironomids and pollen. Engels *et al.* (2018) placed the change to turbid lake-water
410 conditions at 1030 cal. yr. BP, which corresponds to the maximum increase in algae abundances at 185 cm in the
411 pollen data. Our high-resolution record indicates that the first onset of change occurred from 1140 cal. yr. BP
412 onward, with increasing percentages of algae and fungal spores and decreasing pollen percentages of *Littorella*
413 and *Isoëtes* and a shift to brown-green gyttja (Fig.5).

415 The pollen record additionally indicates changes in the regional vegetation during the investigated
416 period, with a reforestation phase in zone Pb from 1730 till 1270 cal. yr. BP (Fig. 5). These regional changes in
417 forest cover did not result in significant changes in the aquatic vegetation in the lake during Ch1. It is possible that
418 the presence of a slightly raised area surrounding Lake Uddelermeer, as seen on the LIDAR elevation map (Fig.
419 1), limited inflow of surface water runoff into the lake from the surrounding area, limiting the impact of regional
420 changes in land use. Increased sediment and nutrient input into the lake as a result of agriculture and
421 deforestation are often the main actor in ecosystem changes in lakes. Potito *et al.* (2014) identified agricultural
422 land cover as one of the most dominant environmental variables influencing chironomid composition.
423 Nevertheless, chironomid inferred temperatures can still be valid from these lakes when agriculture remained
424 stable during the investigated time period (Potito *et al.* 2014). From the pollen record the presence of agriculture
425 in the area was evident, albeit in low percentages which remained constant in pollen zones Pa and Pb and only
426 slightly increased during Pc. In addition, consistently high lake levels are reconstructed for the investigated period
427 (Engels *et al.* 2016), suggesting that changes in water level, which could also affect the chironomid assemblages
428 (Engels and Cwynar 2011), did not play a role either. We therefore conclude that environmental conditions in the
429 lake remained stable in the period between 2525 cal. yr. BP and 1140 cal. yr. BP and suggest that the chironomid
430 record could provide a reliable temperature reconstruction for this period. The chironomid fauna that was existent
431 during the formation of the upper samples (220-100 cm depth), obtained from the green algal gyttja (Ch2), was
432 strongly influenced by the local eutrophication process. These samples are therefore deemed unreliable for
433 temperature reconstruction purposes and will not be discussed.

434

435 *Figure 6 around here*

436

437 **4.5 Chironomid-inferred mean July air temperature reconstruction**

438 Reconstructed mean July air temperature values vary between 16.1 and 19.1°C with an average
439 reconstructed temperature of 17.6°C (Fig. 6). This places the reconstruction in the upper part of the temperature
440 range of the calibration dataset (3.5-18.4 °C) (Heiri *et al.* 2011). Sample-specific errors range between 1.4 and 1.6
441 °C.

442 A number of temperature fluctuations can be observed between 2525 and 1140 cal. yr. BP. At the start
443 of the investigated period (2525-2240 cal. yr. BP, or 550-470 cm depth), mean July air temperature values are
444 low, with an average temperature of 17.4°C. For the period between 2240 and 1760 cal. yr. BP (470-390 cm),
445 slightly higher temperatures are reconstructed, with an average temperature of 18.6°C. Maximum reconstructed
446 temperatures of 19.1°C are reached at a depth of 464 cm (2197 cal. yr. BP). Slightly colder conditions, with an
447 average mean July air temperature of 17.1°C, prevailed in the period between 1760 and 1280 cal. yr. BP (390-
448 255 cm). The coldest phase is reconstructed from 330-304 cm (1551-1465 cal. yr. BP) with an average mean July
449 air temperature of only 16.5°C. This is followed by slightly higher (average 18.3°C) values for the period between
450 1280 and 1140 cal. yr. BP (255-220 cm).

451 The down-core evaluation analyses suggest that most chironomid assemblages in the fossil record are
452 classified as having both 'no close' or 'no good' modern analogue and a 'poor' or 'very poor' fit with temperature.
453 Only two samples contain taxa which are not included in the calibration dataset, reaching values of maximum 2%.
454 Therefore, even though the composition of the chironomid assemblages in the fossil record differs from the
455 modern assemblages, the individual taxa in the fossil samples are well represented in the modern samples. WA-
456 PLS can perform relatively well in no-analogue conditions as long as the majority of the chironomid assemblage is
457 well represented in the calibration data set (Birks 1998).

458 Reconstructed mean July air temperatures in part, exceed the maximum mean July air temperature of
459 the modern samples in the calibration dataset of 18.4 °C. This might have affected the absolute values of the
460 temperature reconstruction. The magnitude of the observed fluctuations (1.39-1.56 °C) is similar to the sample-
461 specific error of the reconstructed temperatures. Nevertheless, the fluctuations are recorded in multiple samples
462 on a high temporal resolution, thus giving a consistent picture of these temperature changes. Moreover, observed
463 fluctuations approximately coincide with shifts in the chironomid assemblage. For example, during the two colder
464 oscillations, taxa with relatively low optimum temperatures are present, such as *Limnophyes/Paralimnophyes*,
465 *Procladius* and *P. sordidellus*. Similarly, the sample with the highest reconstructed mean July air temperature
466 (464 cm) coincides with maximum abundances of *E. albipennis*-type, which is found in the warmer lakes of the
467 calibration dataset (Heiri *et al.* 2011) suggesting that temperature is indeed the main driver of the chironomid
468 fauna in this part of the record. When we compare the reconstructed C-IT from Lake Uddelermeer to the average
469 July temperature of 17 °at de Bilt (50 km SW of Lake Uddelermeer) for the period 1901-2017 it seems that our
470 reconstructed temperatures are relatively high. Even during the DACP reconstructed temperatures are similar to
471 recent conditions (17 °C vs. 17.1°C) indicating that the record is likely overestimating the absolute temperature.
472 Potito *et al.* (2014) found that sites with agriculture in their catchment can overestimate temperature as a result of
473 increased production in the lake. Other chironomid records from NW Europe also indicate that temperature during
474 the DACP was at least 1°C lower than current temperature values (Northern England: Langdon *et al.* 2004;
475 Barber *et al.* 2013; Cairngorms UK: Dalton *et al.* 2005; northern Alps: Millet *et al.* 2009). Additionally, the
476 reconstructed temperature range is located in the upper ranges of the Norwegian/Alpine training set which could
477 result in so called edge-effects. It therefore seems likely that the absolute values of our C-IT reconstruction
478 overestimate past July air temperatures.

479

480 **5 Discussion**

481 Based on the chronology of the record, we can correlate the observed temperature oscillations in the
482 record to climate fluctuations as recorded in the Northern Hemisphere (e.g. Ljungqvist 2010). The slightly higher
483 reconstructed temperatures in the period from 2240-1760 cal. yr. BP probably correspond with the RWP. The
484 subsequent cold phase (1760-1280 cal. yr. BP) can be correlated to the DACP. The warmer conditions
485 reconstructed for the upper part of the record (1280-1140 cal. yr. BP) can be linked to the MCA (Fig. 6). The C-IT
486 record shows that temperature during the Iron Age (till 2240 cal. yr. BP) was lower than during the RWP by an
487 estimated 1.2 °C. To evaluate the representability of these temperature trends in NW Europe we will first compare
488 our results to other C-IT records. In a second step we will compare our results to other available climate
489 reconstructions from NW Europe including detailed tree-ring records and global data compilations.

490

491 *Figure 7 around here*

492

493 **5.1 Chironomid-inferred temperature reconstructions from NW Europe**

494 To our knowledge only two other Late Holocene C-IT reconstructions, which have been identified as
495 representative NW-European temperature trends for the period discussed here, are available. Both of these sites
496 are located in Northern England: Talkin Tarn (Langdon *et al.* 2004) and Bigland Tarn (Barber *et al.* 2013). A RWP,
497 a distinct DACP and the MCA can be distinguished in the record from Bigland Tarn (Fig. 7). These phases might
498 also be visible in the record from Talkin Tarn, although the comparison with that record is less robust, due to the
499 lower sampling resolution and uncertain chronology of that site. The similarity between the three sites, both in
500 timing as well as amplitude of temperature change, suggests that the reconstructed temperature fluctuations in
501 Lake Uddelermeer record reflect a regional climate signal. The overall trend of the reconstruction from
502 Uddelermeer is very similar to that of Bigland Tarn and Talkin Tarn. The RWP is the warmest phase in the
503 Uddelermeer record with an increase in temperature of 1.2 °C compared to the Iron Age. This is similar to the
504 increase in the Bigland Tarn record of 1°C. The average temperature drop from the RWP to the DACP in the
505 Uddelermeer record is 1.5 °C whereas this shift in the Bigland Tarn record is slightly bigger with 2.2 °C. The MCA
506 forms the warmest period in the Bigland Tarn record with an average temperature of 13.7°C. The MCA in the
507 Uddelermeer is only partly present and as seen in the Bigland Tarn record, the first part is not the warmest part of
508 the period. When we compare absolute values of the independent reconstructions, it becomes apparent that
509 reconstructed temperatures from both sites in England are consistently lower by 4-5 °C than the reconstruction
510 from Lake Uddelermeer (Fig. 7). This could in part be the result of the more western location and higher elevation
511 of these sites. The current average July temperatures of both Bigland Tarn as Talkin Tarn are around 15°C,
512 compared to the average July temperature of 17°C at Uddelermeer. Additionally, previous studies have shown
513 that the application of different chironomid-climate calibration datasets to the same fossil record will yield C-IT
514 records that are up to several degrees different in absolute reconstructed temperatures (e.g. Engels *et al.* 2014;
515 Bajolle *et al.* 2018). The temperature reconstructions from England are based on the Norwegian calibration
516 dataset, which has a lower maximum temperature (16 °C; Brooks and Birks 2000) than the extended and
517 combined Swiss-Norwegian dataset used for the reconstruction from Uddelermeer (18.4 °C; Heiri *et al.* 2011).
518 However, it is likely that a large part of the difference in absolute temperatures is the result of a temperature
519 overestimation in the record from Lake Uddelermeer.

520

521 *Figure 8 around here*

522

523 **5.2 Regional evidence from the NH for the RMP, DACP and MCA**

524 When we compare the start and end dates of the climatic phases identified in the record from
525 Uddelermeer to other temperature reconstructions and overviews from the Northern Hemisphere we observe that
526 overall there is a good match between the available records (Fig. 8). All datasets shown in Fig. 8 show a similar
527 starting date for the MCA, which is placed around 1300 cal. yr. BP. The start of the DACP shows slightly more
528 variation in timing with starting dates ranging between 1536-1760 cal. yr. BP. Taking into account all age
529 uncertainties it is likely that all records and overviews show the same simultaneous event. The start of the DACP
530 in Uddelermeer is the earliest of the available estimates with a suggested starting date of 1760 cal. yr. BP. The
531 500-year duration of the DACP in the Uddelermeer record is 150 years longer than the duration of the DACP in
532 the tree-ring record presented by Büntgen *et al.* (2011).

533 The latter part of the DACP in the tree-ring record of Büntgen *et al.* (2011) dated at 1414-1290 cal. yr. BP
534 (536-660 AD) was later termed the Late Antique Little Ice Age or LALIA (Büntgen *et al.* 2016). This LALIA shows
535 a strong temperature decline and is causally linked to a cluster of volcanic eruptions in 1414; 1410 and 1403 cal.
536 yr. BP (536, 540 and 547 AD). Büntgen *et al.* (2017) promote the substitution of the DACP by the LALIA.
537 However, the LALIA has not been identified in a large range of proxies and sites, and falls within the previously
538 defined DACP. Additionally, since the timing and the causality differ, with a link to volcanism for the LALIA and an
539 unknown cause for the DACP, the LALIA cannot be used as a substitution of the DACP. It therefore seems more
540 appropriate to refer to this cold stage as a whole as the DACP (*sensu* Helama *et al.* 2017b; Helama *et al.* 2017a).
541 The Uddelermeer record does suggest a colder second part of the DACP which starts at 1550 cal. yr. BP and
542 lasts till 1450 cal. yr. BP. It is possible that this colder phase reflects the LALIA, although the chronology of the
543 cold period observed in our Uddelermeer record does not match the timing and duration observed in the tree ring
544 record (Büntgen *et al.* 2017). More detailed and well-dated studies covering this time period would contribute to a
545 better understanding of this coldest phase of the DACP.

546 An earlier start and a longer duration of the DACP in the Netherlands, compared to the DACP recorded
547 in the tree ring record, could be the result of different local climatic conditions. Nevertheless, a longer and earlier
548 DACP is in line with both the Bigland Tarn record as well as the two overview studies by Ljunqvist (2009) and
549 Helama (2017). Aside from the tree-ring data set, the Uddelermeer chironomid record is the most detailed
550 temperature record reconstructing absolute temperature values during the Dark Ages Cold Period in for NW
551 Europe.

552 The start of the RWP cannot be identified in all studies presented in Fig. 8. In the Bigland Tarn and
553 Uddelermeer records the start of the RWP is placed at 2365 cal. yr. BP and 2240 cal. yr. BP, respectively. Taking
554 into account the error margins of the chronology of both studies, this could be a simultaneous event. In the tree-
555 ring data set no clear RWP is evident, but the start of a warmer phase does coincide with the start of the RWP at
556 Uddelermeer. However, this warm period as identified in the tree ring record (Büntgen *et al.* 2016) is interrupted
557 by a colder phase. The reconstructed temperatures in Uddelermeer and Bigland Tarn are both stable during the
558 RWP and show no evidence of a brief colder period. The most probable explanation for this discrepancy are
559 different climatic conditions in the Alps in contrast to the lower lying sites, as well as differences in sampling
560 resolution and proxy sensitivity. In the chironomid record from the northern French Alps by Millet *et al.* (2009),
561 which is not interpreted as a representative temperature reconstruction for the first millennium, also no clear RWP
562 was visible. Different climatic conditions might also explain the differences in duration and the start of the DACP
563 across the European continent. Overall, the start and end dates of the different climatic phases fall within the
564 dating uncertainties and current results indicate that especially the MCA and DACP and to a lesser extent the
565 RWP can be considered as simultaneous events across NW Europe.

566

567 **6 Conclusions**

568 We presented the first high-resolution chironomid record for the late Subatlantic in the Netherlands from
569 Lake Uddelermeer. Our data shows that in the period 2500 to 1140 cal. yr. BP the lake was mesotrophic with
570 clear-water conditions and sustained a *Littorellion*. From 1140 cal. yr. BP onward a shift in the water quality was
571 reconstructed with high-nutrient turbid conditions and a dominance of algal species. The conditions in the lake in
572 the period 2500-1140 cal. yr. BP do not signal large ecological changes or effects of human impact and thus
573 suggest that this record is suitable for a temperature reconstruction. In this C-IT record from Lake Uddelermeer,
574 we identified a RWP, a DACP and the MCA. The RWP is placed in the period from 2240-1760 cal. yr. BP, the
575 DACP starts at 1760 cal. yr. BP and the MCA starts at 1280 cal. yr. BP. Our detailed summer temperature record
576 shows that the average temperature drops by 1.5°C from the RWP to the DACP. Overall the temperature
577 reconstructions appears to be too high, however, the trends, temperature fluctuations and timing of the cold and
578 warm periods in this records are in agreement with other records and reconstructions indicating that the
579 Uddelermeer record can be used as an representative record for temperature in the Netherlands during the first
580 millennium AD.

581

582 **Acknowledgements**

583 This work is part of the project "The Dark Age of the Lowlands in an interdisciplinary light: people,
584 landscape and climate in the Netherlands between AD 300 and 1000" (NWO, section Humanities; 2012-2019:
585 360-60-110; www.darkagesproject.com). Loss on Ignition measurements were executed by T. Winkels and an
586 initial low-resolutions set of chironomid samples were analysed by M. Wolma. The chironomid data was
587 transferred to a temperature reconstruction by O. Heiri. We thank Keith Barber, who sadly passed away, for
588 providing the chironomid data of Bigland Tarn and Talkin Tarn. The authors would like to thank H. Middelkoop
589 and O. Heiri for useful comments on the paper. We thank T. Poelen and Kroondomein Het Loo for granting
590 access to the site.

591

592 **References**

- 593 AHN Actueel Hoogtebestand Nederland. www.ahn.nl; www.nationaalgeoregister.nl.
- 594 Archeologisch Basis Register (ABR) in Nationale Onderzoeksagenda Archeologie (NOaA). (2016) Rijksdienst
595 Cultureel Erfgoed. <https://archeologieinnederland.nl/bronnen-en-kaarten/noaa>. Accessed 01-08-2018
- 596 Axford Y., Geirsdóttir Á., Miller G.H., Langdon P.G. (2009) Climate of the Little Ice Age and the past 2000 years in
597 northeast Iceland inferred from chironomids and other lake sediment proxies. *Journal of Paleolimnology*
598 41:7-24 doi:<https://doi-org.proxy.library.uu.nl/10.1007/s10933-008-9251-1>
- 599 Bajolle L., Larocque-Tobler I., Gandouin E., Lavoie M., Bergeron Y., Ali A.A. (2018) Major postglacial summer
600 temperature changes in the central coniferous boreal forest of Quebec (Canada) inferred using
601 chironomid assemblages. *Journal of Quaternary Science* 33:409-420 doi:<https://doi.org/10.1002/jqs.3022>
- 602 Barber K., Brown A., Langdon P., Hughes P. (2013) Comparing and cross-validating lake and bog palaeoclimatic
603 records: A review and a new 5,000 year chironomid-inferred temperature record from northern England.
604 *Journal of Paleolimnology* 49:497-512 doi:<https://doi-org.proxy.library.uu.nl/10.1007/s10933-012-9656-8>
- 605 Beug H.-J. (2004) Leitfaden der pollenbestimmung, für Mitteleuropa und angrenzende Gebiete. Fischer,
606 Stuttgart:542 p.
- 607 Birks H.J.B. (1998) Numerical tools in palaeolimnology-Progress, potentialities, and problems. *Journal of*
608 *Paleolimnology* 20:307-332
- 609 Birks H.J.B., Ter Braak C.J.F., Line J.M., Juggins S., Stevenson A.C. (1990) Diatoms and pH reconstruction. *Phil*
610 *Trans R Soc Lond B* 327:263-278

611 Bohncke S.J.P. (1999) Verslag betreffende het onderzoek naar de archiefwaarde van de sedimenten van het
612 Uddelermeer. Vrije Universiteit Amsterdam, Amsterdam

613 Brodin Y.W. (1986) The postglacial history of Lake Flarken, southern Sweden, interpreted from subfossil insect
614 remains. *Internationale Revue der gesamten Hydrobiologie und Hydrographie* 71:371-432

615 Bronk Ramsey C. (2009) Bayesian analysis of radiocarbon dates. *Radiocarbon* 51:337-360

616 Brooks S.J., Axford Y., Heiri O., Langdon P.G., Larocque-Tobler I. (2012) Chironomids can be reliable proxies for
617 Holocene temperatures. A comment on Velle et al. (2010). *The Holocene* 22:1495-1500 doi:[https://doi-
618 org.proxy.library.uu.nl/10.1177/0959683612449757](https://doi-org.proxy.library.uu.nl/10.1177/0959683612449757)

619 Brooks S.J., Birks H.J.B. (2000) Chironomid-inferred late-glacial and early-Holocene mean July air temperatures
620 for Kråkenes Lake, western Norway. *Journal of Paleolimnology* 23:77-89

621 Brooks S.J., Langdon P.G., Heiri O. (2007) The identification and use of Palaeartic Chironomidae larvae in
622 palaeoecology. QRA Technical guide No. 10. Quaternary Research Association, London

623 Bunnik F.P.M. (1999) Vegetationsgeschichte der Lößböden zwischen Rhein und Maas von der Bronzezeit bis in
624 die frühe Neuzeit., Utrecht University

625 Büntgen U., Myglan V.S., Ljungqvist F.C., McCormick M., Di Cosmo N., Sigl M., Jungclaus J., Wagner S., Krusic
626 P.J., Esper J. (2017) Reply to 'Limited Late Antique cooling'. *Nature Geoscience* 10:243

627 Büntgen U., Myglan V.S., Ljungqvist F.C., McCormick M., Di Cosmo N., Sigl M., Jungclaus J., Wagner S., Krusic
628 P.J., Esper J., Kaplan J.O., de Vaan M.A.C., Luterbacher J., Wacker L., Tegel W., Kirilyanov A.V. (2016)
629 Cooling and societal change during the Late Antique Little Ice Age from 536 to around 660 AD. *Nature*
630 *Geosci* 9:231-236 doi:<https://doi.org/10.1038/NGEO2652>

631 Büntgen U., Tegel W., Nicolussi K., McCormick M., Frank D., Trouet V., Kaplan J.O., Herzig F., Heussner K.U.,
632 Wanner H., Luterbacher J., Esper J. (2011) 2500 years of European climate variability and human
633 susceptibility. *Science* 331:578-582 doi:<https://doi.org/10.1126/science.1197175>

634 Cohen K.M., Toonen W.H.J., Weerts H.J.T. (2016) Overstromingen van de Rijn gedurende het Holocene
635 Relevantie van de grootste overstromingen voor archeologie van het Nederlands rivierengebied.
636 *Deltares*

637 Dalton C., Birks H.J.B., Brooks S.J., Cameron N.G., Evershed R.P., Peglar S.M., Scott J.A., Thompson R. (2005)
638 A multi-proxy study of lake-development in response to catchment changes during the Holocene at
639 Lochnagar, north-east Scotland. *Palaeogeography, Palaeoclimatology, Palaeoecology* 221:175-201
640 doi:<https://doi.org/10.1016/j.palaeo.2005.02.007>

641 Dörfler W., Feeser I., van den Bogaard C., Dreibrödt S., Erlenkeuser H., Kleinmann A., Merkt J., Wiethold J.
642 (2012) A high-quality annually laminated sequence from Lake Belau, Northern Germany: revised
643 chronology and its implications for palynological and tephrochronological studies *The Holocene* 22:1413-
644 1426 doi: <https://doi.org/10.1177/0959683612449756>

645 Engels S., Bakker M.A.J., Bohncke S.J.P., Cerli C., Hoek W.Z., Jansen B., Peters T., Renssen H., Sachse D., van
646 Aken J.M. (2016) Centennial-scale lake-level lowstand at Lake Uddelermeer (The Netherlands) indicates
647 changes in moisture source region prior to the 2.8-kyr event. *The Holocene* 26:1075-1091 doi:[https://doi-
648 org.proxy.library.uu.nl/10.1177/0959683616632890](https://doi-org.proxy.library.uu.nl/10.1177/0959683616632890)

649 Engels S., Bohncke S.J.P., Bos J.A.A., Heiri O., Vandenberghe J., Wallinga J. (2008a) Environmental inferences
650 and chironomid-based temperature reconstructions from fragmentary records of the Weichselian Early
651 Glacial and Pleniglacial periods in the Niederlausitz area (eastern Germany). *Palaeogeography,*
652 *Palaeoclimatology, Palaeoecology* 260:405-416 doi:<https://doi.org/10.1016/j.palaeo.2007.12.005>

653 Engels S., Bohncke S.J.P., Heiri O., Nyman M. (2008b) Intraregional variability in chironomid-inferred temperature
654 estimates and the influence of river inundations on lacustrine chironomid assemblages. *Journal of*
655 *Paleolimnology* 40:129-142 doi:<https://doi-org.proxy.library.uu.nl/10.1007/s10933-007-9147-5>

656 Engels S., Cwynar L.C. (2011) Changes in fossil chironomid remains along a depth gradient: evidence for
657 common faunal thresholds within lakes. *Hydrobiologia* 665:15-38 doi:[https://doi-](https://doi-org.proxy.library.uu.nl/10.1007/s10750-011-0601-z)
658 [org.proxy.library.uu.nl/10.1007/s10750-011-0601-z](https://doi-org.proxy.library.uu.nl/10.1007/s10750-011-0601-z)

659 Engels S., Cwynar L.C., Rees A.B.H., Shuman B.N. (2012) Chironomid-based water depth reconstructions: an
660 independant evaluation of site-specific and local interference models. *Journal of Palaeolimnology*
661 doi:<https://doi-org.proxy.library.uu.nl/10.1007/s10933-012-9638-x>

662 Engels S., Self A.E., Luoto T.P., Brooks S.J., Helmens K.F. (2014) A comparison of three Eurasian chironomid-
663 climate calibration datasets on a W-E continentality gradient and the implications for quantitative
664 temperature reconstructions. *Journal of Paleolimnology* 51:529-547 doi:[https://doi-](https://doi-org.proxy.library.uu.nl/10.1007/s10933-014-9772-8)
665 [org.proxy.library.uu.nl/10.1007/s10933-014-9772-8](https://doi-org.proxy.library.uu.nl/10.1007/s10933-014-9772-8)

666 Engels S., van Oostrom R., Cherli C., Dungait J.A.J., Jansen B., van Aken J.M., van Geel B., Visser P.M. (2018)
667 Natural and anthropogenic forcing of Holocene lake ecosystem development at Lake Uddelermeer (The
668 Netherlands). *Journal of Paleolimnology* 59:329-347 doi:[https://doi-](https://doi-org.proxy.library.uu.nl/10.1007/s10933-017-0012-x)
669 [org.proxy.library.uu.nl/10.1007/s10933-017-0012-x](https://doi-org.proxy.library.uu.nl/10.1007/s10933-017-0012-x)

670 Erkens G. (2009) Sediment dynamics in the Rhine catchment-Quantification of fluvial response to climate
671 change and human impact. *Netherlands Geographical Studies* 388

672 Faegri K., Iversen J. (1989) *Textbook of Pollen Analysis*, revised by Faegri K, Kaland PE, Krzywinski K. J Wiley,
673 New York

674 Farmer A.M., Spence D.H.N. (1986) The growth strategies and distribution of isoetids in Scottish freshwater
675 lochs. *Aquatic Botany* 26:247-258

676 Gräslund B., Price N. (2012) Twilight of the gods? The 'dust veil event' of AD 536 in critical perspective *Antiquity*
677 86:428-443 doi:[doi:10.1017/S0003598X00062852](https://doi.org/10.1017/S0003598X00062852)

678 Grimm E.C. (1991-2015) *Tilia.*, 2.0.41 edn.,

679 Groenewoudt B.J., Schut P.A.C., van der Heijden F.J.G., Peeters H., Wispelwey M.H. (2006) Een inventariserend
680 veldonderzoek bij de Hunneschans (Uddel, Gelderland): nieuwe gegevens over de steentijdbewoning bij
681 het Uddelermeer en een beknopt overzicht van de onderzoeksgeschiedenis van de Hunneschans:
682 Rapportage Archeologische Monumentenzorg 143.

683 Groenewoudt B.J., van Lanen R.J. (2018) Diverging decline. Reconstructing and validating (post-)Roman
684 population trends (AD 0-1000) in the Rhine-Meuse delta (the Netherlands). *Post Classical Archaeologies*
685 8:30

686 Hannon G.E., Gaillard M.-J. (1997) The plant-macrofossil record of past lake-level changes. *Journal of*
687 *Paleolimnology* 18:15-28

688 Heidinga H.A. (1987) *Medieval Settlement and Economy North of the Lower Rhine: Archeology and History of*
689 *Kootwijk and the Veluwe (the Netherlands)*. Van Gorcum Ltd,

690 Heiri O., Brooks S.J., Birks H.J.B., Lotter A.F. (2011) A 274-lake calibration data-set and inference model for
691 chironomid-based summer air temperature reconstruction in Europe. *Quaternary Science Reviews*
692 30:3445-3456 doi:<https://doi.org/10.1016/j.quascirev.2011.09.006>

693 Heiri O., Brooks S.J., Renssen H., Bedford A., Hazekamp M., Ilyashuk B., Jeffers E.S., Lang B., Kirilova E.,
694 Kuiper S. (2014) Validation of climate model-inferred regional temperature change for late-glacial
695 Europe. *Nature communications* 5:4914 doi:<https://doi.org/10.1038/ncomms5914>

696 Heiri O., Lotter A.F., Lemcke G. (2001) Loss on ignition as a method for estimating organic and carbonate content
697 in sediments: reproducibility and comparability of results. *Journal of Paleolimnology* 25:101-110

698 Helama S., Jones P.D., Briffa K.R. (2017a) Dark Ages Cold Period: A literature review and directions for future
699 research. *The Holocene* 27:1600-1606 doi:<https://doi.org/10.1177/0959683617693898>

700 Helama S., Jones P.D., Briffa K.R. (2017b) Limited Late Antique cooling. *Nature Geoscience* 10:242

701 Jansma E., Gouw-Bouman M.T.I.J., Van Lanen R.J., Pierik H.J., Cohen K.M., Groenewoudt B.J., Hoek W.Z.,
702 Stouthamer E., Middelkoop H. (2014) The Dark Age of the Lowlands in an interdisciplinary light: people,
703 landscape and climate in The Netherlands between AD 300-1000. *European Journal of Post-Classical*
704 *Archaeologies (PCA 4):471-476*

705 Kalis A.J., Karg S., Meurers-Balke H., Teunissen-van OOrschot H. (2008) Mensch und Vegetation am Unteren
706 Niederrhein wahren der Eisen- und Romerzeit. In: Muller M, Schalles H-J, Zieling N (eds) *Colonia Ulpia*
707 *Traiana, Xanten und sein Umland in romischer Zeit, Xantener Berichte, Geschichte der Stadt Xanten.*,
708 vol 1. pp 31-48

709 Knol E. (1993) *De Noordnederlandse kustlanden in de Vroege Middeleeuwen.*, VU University Amsterdam

710 Kraanen C.J.M., Pape J.C. (1965) *De bodemgesteldheid van de omgeving van het Uddelermeer.* STIBOKA,

711 Langdon P.G., Barber K.E., Lomas-Clarke S.H. (2004) Reconstructing climate and environmental change in
712 northern England through chironomid and pollen analyses: evidence from Talkin Tarn, Cumbria. *Journal*
713 *of Palaeolimnology 32:197-203*

714 Langdon P.G., Ruiz Z., Brodersen K.P., Foster I.D.L. (2006) Assessing lake eutrophication using chironomids:
715 understanding the nature of community response in different lake types. *Freshwater biology 51:562-577*
716 doi:<https://doi.org/doi:10.1111/j.1365-2427.2005.01500.x>

717 Larsen L.B., Vinther B.M., Briffa K.R., Melvin T.M., Clausen H.B., Jones P.D., Siggaard-Andersen M.L., Hammer
718 C.U., Eronen M., Grudd H., Gunnarson B.E., Hantemirov R.M., Naurzbaev M.M., Nicolussi K.C.L. (2008)
719 New ice core evidence for a volcanic cause of the A.D. 536 dust veil. *Geophysical Research Letters*
720 *35:n/a-n/a* doi:<https://doi-org.proxy.library.uu.nl/10.1029/2007GL032450>

721 Litt T., Scholzel C., Kuhl N., Brauer A. (2009) Vegetation and climate history in the Westeifel Volcanic Field
722 (Germany) during the past 11 000 years based on annually laminated lacustrine maar sediments.
723 *Boreas 38:679-690* doi:<https://doi.org/10.1111/j.1502-3885.2009.00096.x>

724 Ljungqvist F.C. (2009) Temperature proxy records covering the last two millennia: a tabular and visual overview.
725 *Geografiska Annaler: Series A, Physical Geography 91:11-29* doi:[https://doi.org/10.1111/j.1468-](https://doi.org/10.1111/j.1468-0459.2009.00350.x)
726 [0459.2009.00350.x](https://doi.org/10.1111/j.1468-0459.2009.00350.x)

727 Ljungqvist F.C. (2010) A new reconstruction of temperature variability in the extra-tropical northern hemisphere
728 during the last two millennia. *Geografiska Annaler, series A:339-351*

729 Luoto T.P. (2011) The relationship between water quality and chironomid distribution in Finland—a new
730 assemblage-based tool for assessments of long-term nutrient dynamics. *Ecological Indicators 11:255-*
731 *262* doi:<https://doi.org/10.1016/j.ecolind.2010.05.002>

732 Luoto T.P. (2012) Intra-lake patterns of aquatic insect and mite remains. *Journal of Paleolimnology 47:141-157*
733 doi:<https://doi-org.proxy.library.uu.nl/10.1007/s10933-011-9565-2>

734 McCormick M., Buntgen U., Cane M.A., Cook E.R., Harper K., Huybers P., Litt T., Manning S.W., Mayewski P.A.,
735 More A.F.M., Nicolussi K., Tegel W. (2012) Climate Change during and after the Roman Empire:
736 Reconstructing the Past from Scientific and Historical Evidence. *Journal of Interdisciplinary History*
737 *43:169-220*

738 McKeown M., Potito A.P. (2016) Assessing recent climatic and human influences on chironomid communities
739 from two moderately impacted lakes in western Ireland. *Hydrobiologia 765:245-263* doi:[https://doi-](https://doi-org.proxy.library.uu.nl/10.1007/s10750-015-2418-7)
740 [org.proxy.library.uu.nl/10.1007/s10750-015-2418-7](https://doi-org.proxy.library.uu.nl/10.1007/s10750-015-2418-7)

741 Millet L., Arnaud F., Heiri O., Magny M., Verneaux V., Desmet M. (2009) Late-Holocene summer temperature
742 reconstruction from chironomid assemblages of Lake Anterne, northern French Alps. *The Holocene*
743 *19:317-328* doi:<https://doi.org/10.1177/0959683608100576>

744 Moller Pillot H.K.M. (1984a) *De Larven der Nederlandse Chironomidae (Diptera): Orthocladiinae sensu lato.*
745 *Nederlandse Faunistische Mededelingen 1:1-175*

746 Moller Pillot H.K.M. (1984b) De larven der Nederlandse Chironomidae (Diptera); (Inleiding, Tanypodinae &
747 Chironomini). Nederlandse Faunistische Mededelingen 1:1-277

748 Moller Pillot H.K.M. (2013) Chironomidae Larvae of the Netherlands and adjacent lowlands: biology and ecology
749 of the chironomini. KNNV publishing,

750 Moller Pillot H.K.M., Klink A.G. (2009) Chironomidae larvae. Biology and Ecology of the Chironomini KNNV
751 Publishing, Zeist

752 Moore P.D., Webb J.A., Collison M.E. (1991) Pollen analysis. Blackwell scientific publications,

753 Nazarova L., de Hoog V., Hoff U., Dirksen O., Diekmann B. (2013) Late Holocene climate and environmental
754 changes in Kamchatka inferred from the subfossil chironomid record. Quaternary Science Reviews
755 67:81-92 doi:<https://doi.org/10.1016/j.quascirev.2013.01.018>

756 Padisák J., Krienitz L., Scheffler W., Koschel R., Kristiansen J., Grigorszky I. (1998) Phytoplankton succession in
757 the oligotrophic Lake Stechlin (Germany) in 1994 and 1995 Hydrobiologia 369:179-197

758 Pierik H.J. (2017) Past human-landscape interactions in the Netherlands: Reconstructions from sand belt to
759 coastal-delta plain for the first millennium AD. vol 139. Utrecht studies in earth sciences. Utrecht
760 University,

761 Pierik H.J., Cohen K.M., Stouthamer E. (2016) A new GIS approach for reconstructing and mapping dynamic late
762 Holocene coastal plain palaeogeography. Geomorphology 270:55-70
763 doi:<http://dx.doi.org/10.1016/j.geomorph.2016.05.037>

764 Pierik H.J., Stouthamer E., Cohen K.M. (2017) Natural levee evolution in the Rhine-Meuse delta, the Netherlands,
765 during the first millennium CE. Geomorphology 295:215-234
766 doi:<https://doi.org/10.1016/j.geomorph.2017.07.003>

767 Pierik H.J., van Lanen R.J. (2017) Roman and early-medieval habitation patterns in a delta landscape: The link
768 between settlement elevation and landscape dynamics. Quaternary International
769 doi:<https://doi.org/10.1016/j.quaint.2017.03.010>

770 Pierik H.J., Van Lanen R.J., Gouw-Bouman M.T.I.J., Groenewoudt B., Wallinga J., Hoek W.Z. (2018) Controls on
771 late Holocene drift-sand dynamics: the role of people and climate on inland aeolian activity in the
772 Netherlands The Holocene 28:1361-1381 doi:<https://doi.org/10.1177/0959683618777052>

773 Koomen A., Maas G. (2004) Geomorfologische Kaart Nederland (GKN); Achtergronddocument bij het
774 landsdekkende digitale bestand. Alterra.

775 Polak B. (1959) Palynology of the "Uddeler Meer". A Contribution to our Knowledge of the Vegetation and of the
776 Agriculture in the Northern Part of the Veluwe in Prehistoric and Early Historic Times. Acta botanica
777 neerlandica 8:547-571

778 Potito A.P., Woodward C.A., McKeown M., Beilman D.W. (2014) Modern influences on chironomid distribution in
779 western Ireland: potential for palaeoenvironmental reconstruction. Journal of Paleolimnology 52:385-404
780 doi:<https://doi-org.proxy.library.uu.nl/10.1007/s10933-014-9800-8>

781 Punt W., Blackmore S., Clarke G.C.S. (1976) The Northwest European pollen flora 1. Elsevier, Amsterdam

782 Punt W., Blackmore S., Clarke G.C.S. (1980) The Northwest European pollen flora 2. Elsevier, Amsterdam

783 Punt W., Blackmore S., Clarke G.C.S. (1981) The Northwest European pollen flora 3. Elsevier, Amsterdam

784 Punt W., Blackmore S., Clarke G.C.S. (1984) The Northwest European pollen flora 4. Elsevier, Amsterdam

785 Punt W., Blackmore S., Clarke G.C.S. (1988) The Northwest European pollen flora 5. Elsevier, Amsterdam

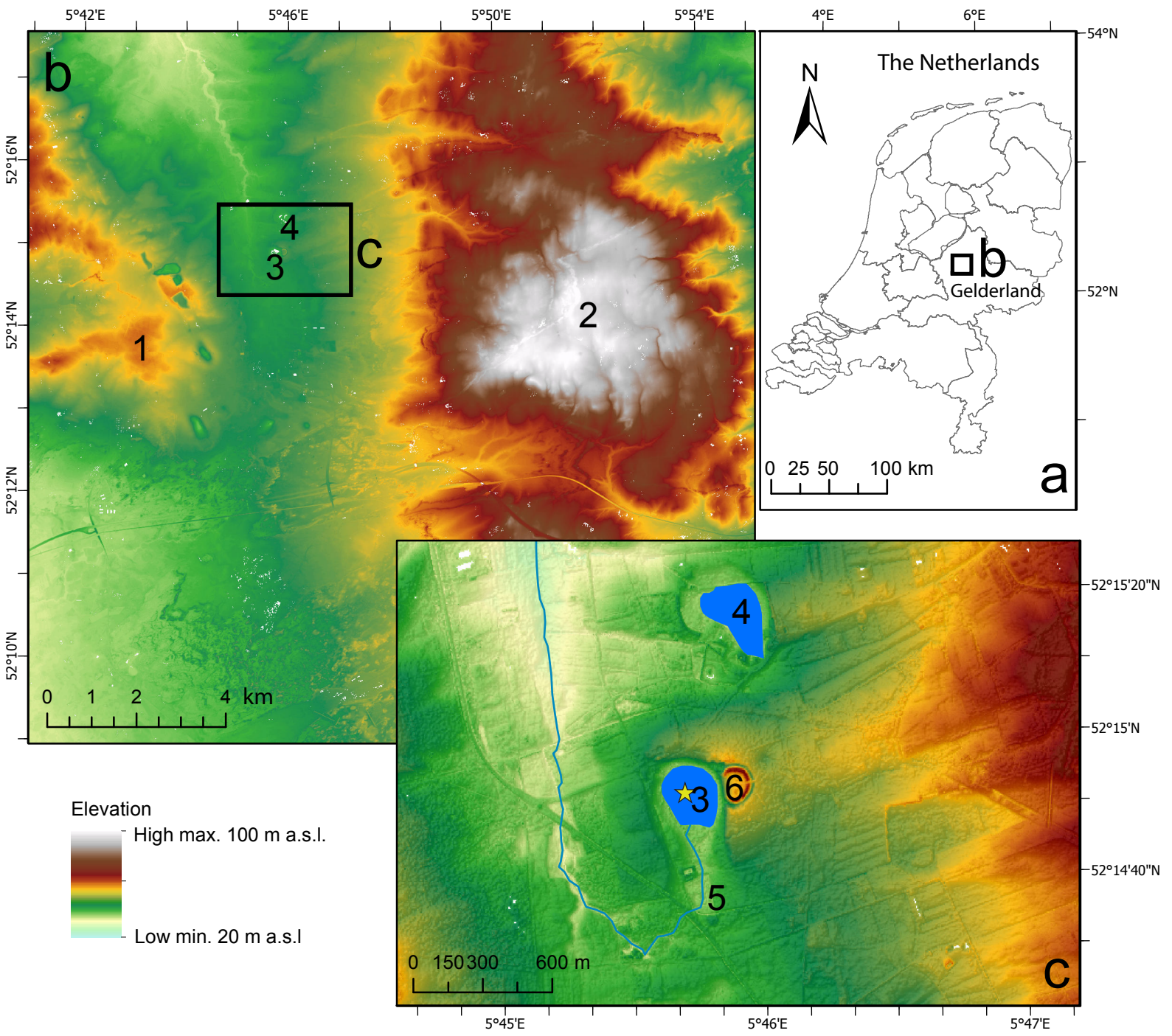
786 Punt W., Blackmore S., Clarke G.C.S. (1991) The Northwest European pollen flora 6. Elsevier,

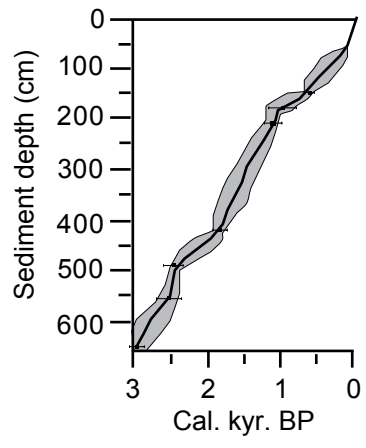
787 Punt W., Blackmore S., Clarke G.C.S. (1995) The Northwest European pollen flora 7. Elsevier,

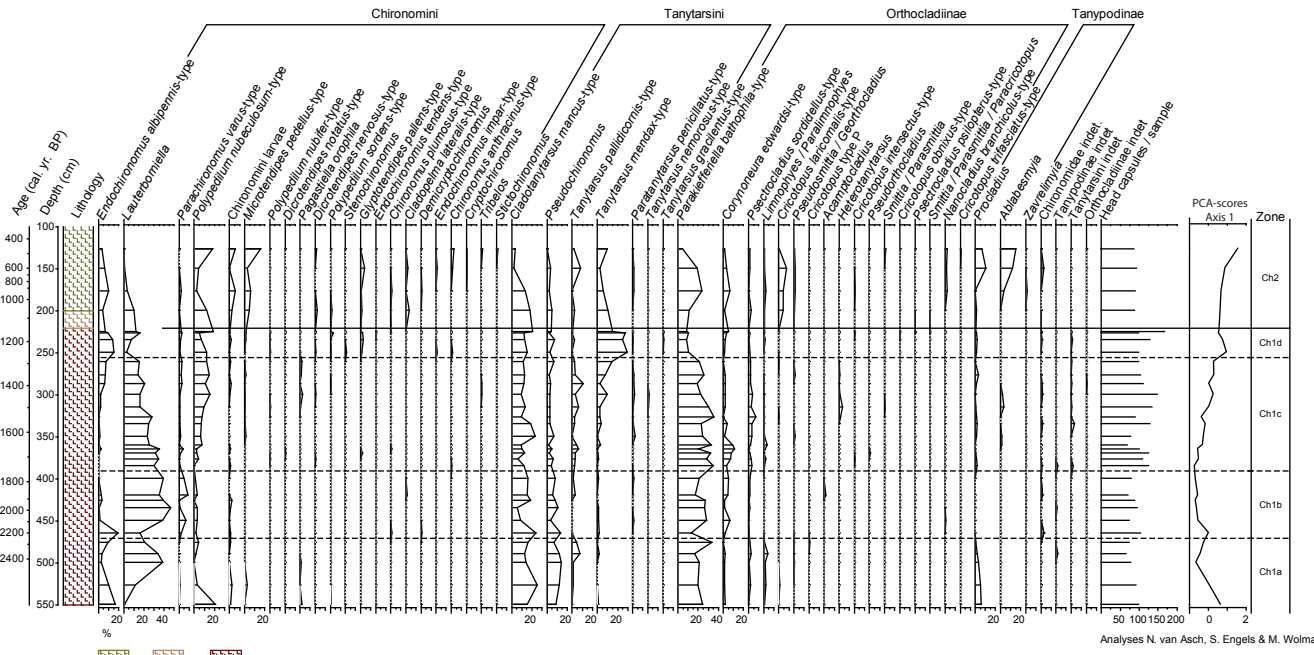
788 Punt W., Blackmore S., Hoen P.P., Stafford P.J. (2003) The Northwest European pollen flora 8. Elsevier,
789 Amsterdam

790 Rasmussen S.O., Andersen K.K., Svensson A.M., Steffensen J.P., Vinther B.M., Clausen H.B., Siggaard-
791 Andersen M.L., Johnsen S.J., Larsen L.B., Dahl-Jensen D., Bigler M., Röhrlisberger R., Fischer H.,
792 Goto-Azuma K., Hansson M.E., Ruth U. (2006) A new Greenland ice core chronology for the last glacial
793 termination. *Journal of Geophysical Research: Atmospheres* 111:n/a-n/a doi:10.1029/2005jd006079
794 Riechelmann D., Gouw-Bouman M.T.I.J. (2019) Climate during the first millennium AD in NW Europe: a review of
795 climate reconstructions from terrestrial archives. *Quaternary Research* 91:111-131
796 doi:<https://doi.org/10.1017/qua.2018.84>
797 Rieradevall M., Brooks S.J. (2001) An identification guide to subfossil Tanypodinae larvae (Insecta: Diptera:
798 Chironomidae) based on cephalic setation. *Journal of Paleolimnology* 25:81-99
799 Roelofs J.G.M., Schuurkes J.A.A.R., Smits A.J.M. (1984) Impact of acidification and eutrophication on
800 macrophyte communities in soft waters. II. Experimental studies. *Aquatic Botany* 18:389-411
801 Rørslett B., Brettum P. (1989) The genus *Isoetes* in Scandinavia: an ecological review and perspectives. *Aquatic*
802 *Botany* 35:223-261
803 Sand-Jensen K. (1978) Metabolic adaptation and vertical zonation of *Littorella uniflora* (L.) Aschers. and *Isoetes*
804 *lacustris* L. *Aquatic Botany* 4:1-10
805 Sohl H. (1983) A palaeo-ecological investigation of the Late Glacial and Holocene lake sediments of the
806 Uddelermeer (The Netherlands): methods and some provisional results. *Quaternary studies in Poland*
807 9:547-571
808 Stouthamer E., Berendsen H.J.A. (2000) Factors Controlling the Holocene Avulsion History of the Rhine-Meuse
809 Delta (The Netherlands). *Journal of Sedimentary Research* 70:1051-1064 doi:10.1306/033000701051
810 Taylor K.J., McGinley S., Potito A.P., Molloy K., Beilman D.W. (2018) A mid to late Holocene chironomid-inferred
811 temperature record from northwest Ireland. *Palaeogeography, Palaeoclimatology, Palaeoecology*
812 505:274-286 doi:<https://doi.org/10.1016/j.palaeo.2018.06.006>
813 Taylor K.J., Potito A.P., Beilman D.W., Ghilardi B., O'Connell M. (2013) Palaeolimnological impacts of early
814 prehistoric farming at Lough Dargan, County Sligo, Ireland. *Journal of Archaeological Science* 40:3212-
815 3221 doi:<https://doi.org/10.1016/j.jas.2013.04.002>
816 Taylor K.J., Potito A.P., Beilman D.W., Ghilardi B., O'Connell M. (2017a) Impact of early prehistoric farming on
817 chironomid communities in northwest Ireland. *Journal of Paleolimnology* 57:227-244
818 doi:<https://doi.org/10.1007/s10933-017-9942-6>
819 Taylor K.J., Stolze S., Beilman D.W., Potito A.P. (2017b) Response of chironomids to Neolithic land-use change
820 in north-west Ireland. *The Holocene* 27:879-889 doi:<https://doi.org/10.1177/0959683616675935>
821 Telford R.J., Birks H.J.B. (2011) A novel method for assessing the statistical significance of quantitative
822 reconstructions inferred from biotic assemblages. *Quaternary Science Reviews* 30:1272-1278
823 doi:<https://doi.org/10.1016/j.quascirev.2011.03.002>
824 ter Braak C.J.F., Šmilauer P. (2012) Canoco reference manual and user's guide: software for ordination, version
825 5.0. Microcomputer power,
826 Teunissen D. (1990) Palynologisch onderzoek in het oostelijk riviereengebied: een overzicht. In: Mededelingen van
827 de afdeling Biogeologie van de Discipline Biologie van de Katholieke Universiteit van Nijmegen. p 16
828 Tinner W., Lotter A.F., Ammann B., Conedera M., Hubschmid P., van Leeuwen J.F.N., Wehrli M. (2003) Climatic
829 change and contemporaneous land-use phases north and south of the Alps 2300 BC to 800 AD.
830 *Quaternary Science Reviews* 22:1447-1460 doi:[https://doi.org/10.1016/S0277-3791\(03\)00083-0](https://doi.org/10.1016/S0277-3791(03)00083-0)
831 Toohey M., Krüger K., Sigl M., Stordal F., Svensen H. (2016) Climatic and societal impacts of a volcanic double
832 event at the dawn of the Middle Ages *Climatic Change* 136:401-412
833 Toonen W.H.J. (2013) A Holocene flood record of the Lower Rhine. Utrecht University

834 Vallenduuk H.J., Moller Pillot H.K.M. (2007) Chironomidae larvae of the Netherlands and adjacent lowlands.
835 KNNV Publishing,
836 van Asch N. (2012) Environmental response to Lateglacial climate change-Reconstructions of temperature and
837 vegetation changes in northwest Europe., Utrecht University
838 van Geel B. (1972) Palynology of a section from the raised bog 'Wietmarscher moor', with special reference to
839 fungal remains. *Plant Biology* 21:261-284
840 van Geel B. (1978) A palaeoecological study of Holocene peat bog sections in Germany and the Netherlands,
841 based on the analysis of pollen, spores and macro-and microscopic remains of fungi, algae,
842 cormophytes and animals. *Review of Palaeobotany and Palynology* 25:1-120
843 van Geel B., Buurman J., Brinkkemper O., Schelvis J., Aptroot A., van Reenen G., Hakbijl T. (2003)
844 Environmental reconstruction of a Roman Period settlement site in Uitgeest (The Netherlands), with
845 special reference to coprophilous fungi. *Journal of Archaeological Science* 30:873-883
846 doi:[https://doi.org/10.1016/S0305-4403\(02\)00265-0](https://doi.org/10.1016/S0305-4403(02)00265-0)
847 Vinther B.M., Clausen H.B., Johnsen S.J., Rasmussen S.O., Andersen K.K., Buchardt S.L., Dahl-Jensen D.,
848 Seierstad I.K., Siggaard-Andersen M.L., Steffensen J.P., Svensson A., Olsen J., Heinemeier J. (2006) A
849 synchronized dating of three Greenland ice cores throughout the Holocene. *Journal of Geophysical*
850 *Research: Atmospheres* 111 doi:10.1029/2005jd006921
851 Vos P.C., Van Heeringen R.M. (1997) Holocene geology and occupation history of the Province of Zeeland
852 *Mededelingen Nederlands Instituut voor Toegepaste Geowetenschappen TNO* 59:5-109
853 Wanner H., Beer J., Bütikofer J., Crowley T.J., Cubasch U., Flückiger J., Goosse H., Grosjean M., Joos F.,
854 Kaplan J.O., Küttel M., Müller S.A., Prentice I.C., Solomina O., Stocker T.F., Tarasov P., Wagner M.,
855 Widmann M. (2008) Mid- to Late Holocene climate change: an overview. *Quaternary Science Reviews*
856 27:1791-1828 doi:<http://dx.doi.org/10.1016/j.quascirev.2008.06.013>
857 Wanner H., Solomina O., Grosjean M., Ritz S.P., Jetel M. (2011) Structure and origin of Holocene cold events.
858 *Quaternary Science Reviews* 30:3109-3123
859 Weeda E.J., Schaminée J.H.J., Van Duuren L. (2000) Atlas van Plantengemeenschappen in Nederland. deel 1:
860 Wateren, moerassen en natte heiden. KNNV Uitgeverij, Utrecht
861 Weeda E.J., Westra R., Westra C., Westra T. (1988) Nederlandse oecologische flora, wilde planten en hun
862 relaties. deel 3. Hilversum
863 Wiederholm T. (1983) Chironomidae of Holarctic region: keys and diagnoses. Part 1. Larvae *Entomol Scand*
864 *Suppl* 19:1-457



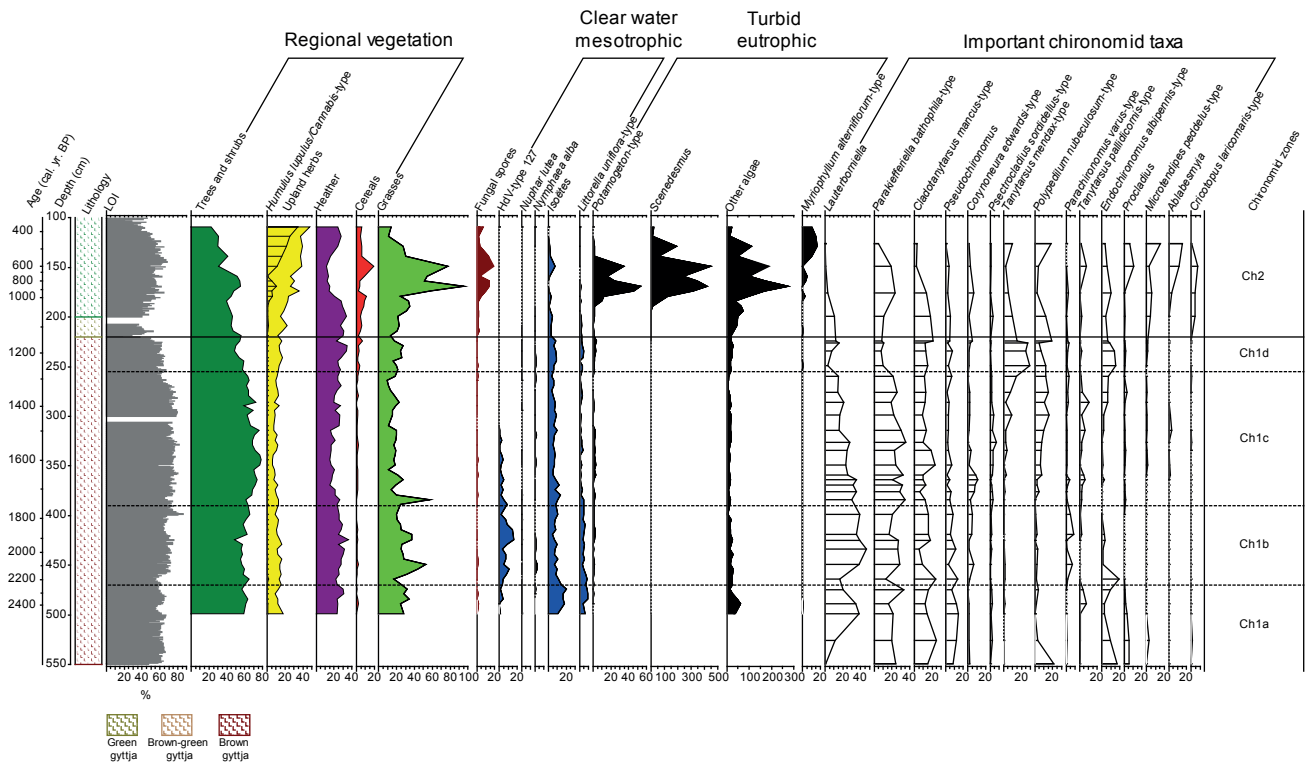


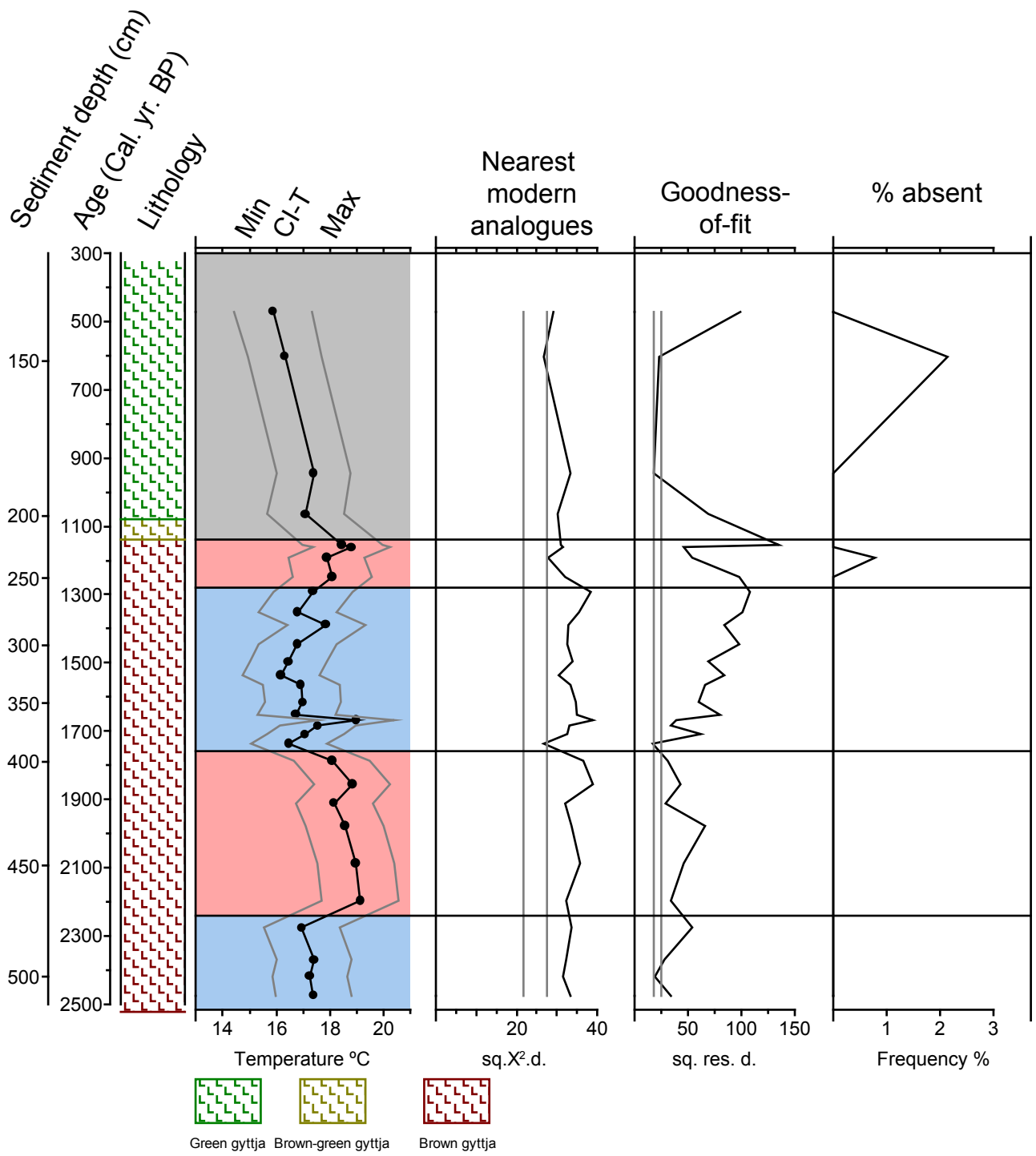


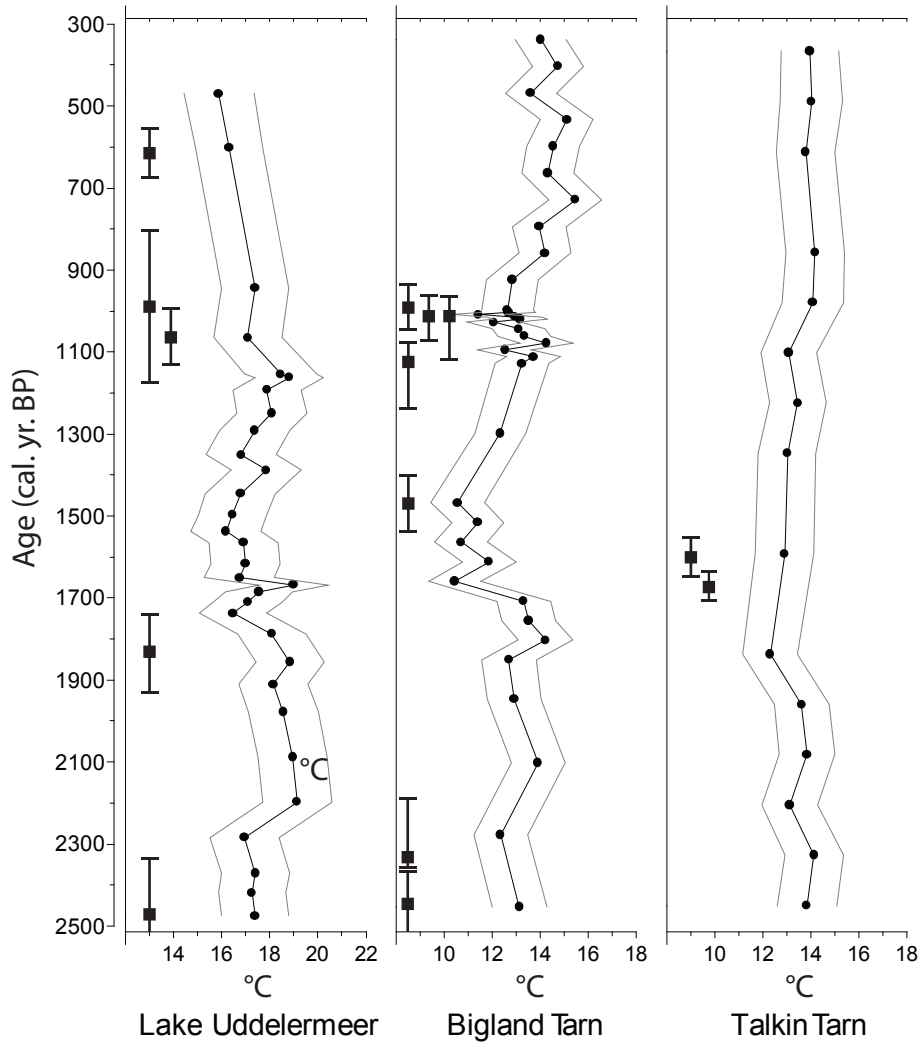
Green
gyttja

Brown-green
gyttja

Brown
gyttja







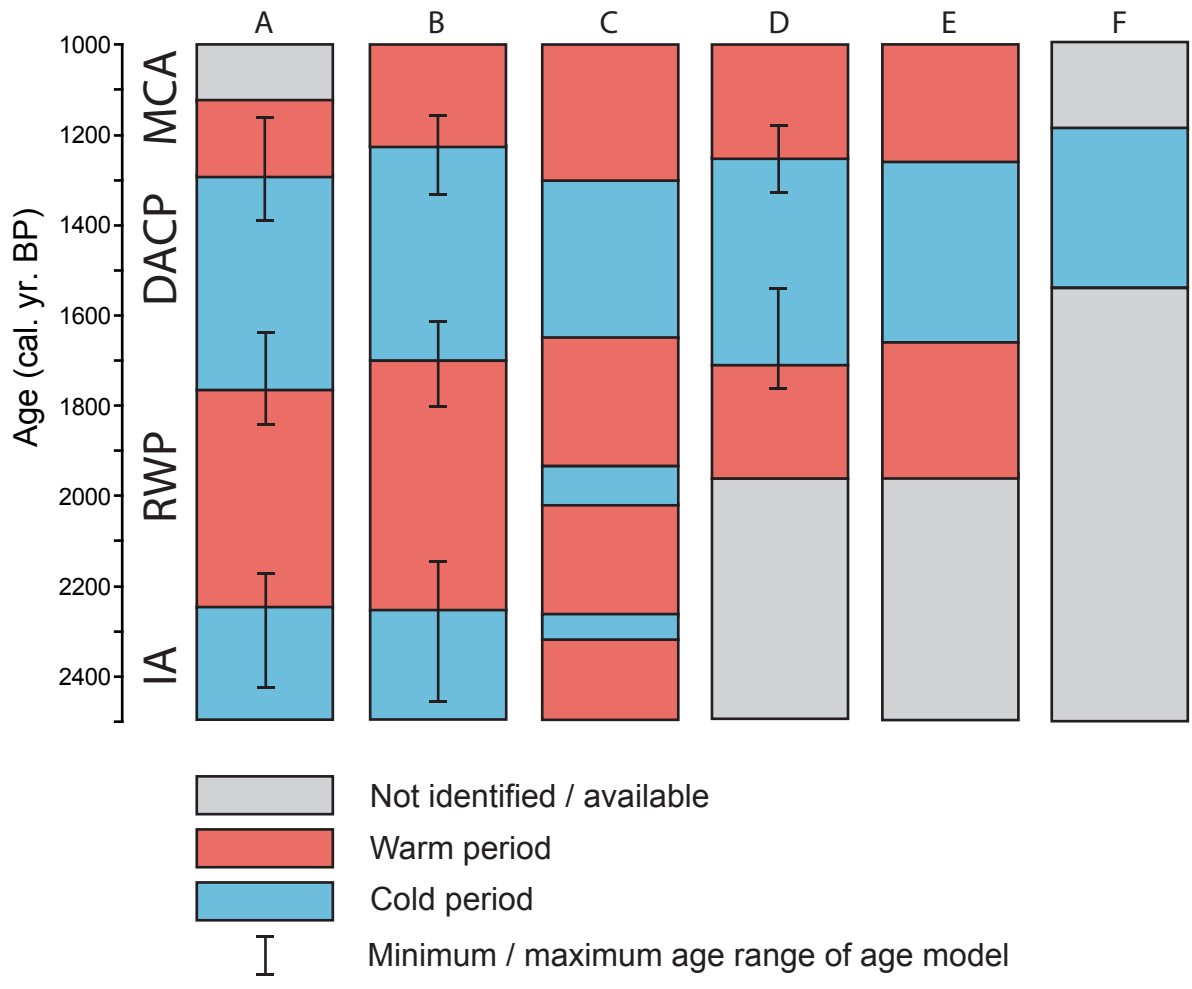


Figure 1 (a) Location of Lake Uddelermeer; (b) Lidar elevation model of the central Netherlands (AHN; www.ahn.nl) and (c) the area directly surrounding Lake Uddelermeer. Yellow star indicates location core. Numbers indicate sites discussed in the text. 1 Ice pushed ridge Garderen-Ermelo max. 50 m A.S.L.; 2 Ice pushed ridge Apeldoorn max. 100 m A.S.L.; 3 Lake Uddelermeer; 4 Lake Bleekemeer; 5 brook Leuvenemse beek; 6 medieval ringfort (ringwalburg) (Koomen & Maas, 2004; Heidinga, 1987). For visibility purposes (c) is plotted with a different colour range, only a relative elevation legend is shown for both maps.

Figure 2 Bayesian modelled age-depth model of core section 50 - 650 cm depth for central Core E from Lake Uddelermeer (figure adapted from Engels et al. (2016)). The 95% probability distribution range is shown in grey, calibrated C^{14} ages and 95% probability ranges are shown as black squares with error bars.

Figure 3 Percentage diagram of selected pollen, spores and NPPs from Lake Uddelermeer showing regional (A) and local (B) vegetation development in and around Lake Uddelermeer. All curves are shown with an additional fivefold exaggeration. Diagram plotted on sediment depth (cm) with a secondary scale (cal. yr. BP) plotted for comparison. Sedimentological and Loss-on-Ignition (represented as organic content% in 3A) profiles are plotted to the left of the pollen curves. The presence of charcoal (indicated with '+' present; '++' present in large quantities) is plotted to the right of the pollen curves.

Figure 4 Percentage diagram showing all chironomid taxa and the chironomid count sum (head capsules/ sample) for Lake Uddelermeer. Diagram plotted on sediment depth (cm) with a secondary scale (cal. yr. BP) plotted for comparison. The sedimentological profile is plotted to the left of the chironomid curves. To the right the scores of the chironomid samples on the first axis of a PCA performed with square-root-transformed percentage data is shown.

Figure 5 Selected percentage curves of pollen, NPPs and chironomid taxa as indicators for regional vegetation change, lake ecology and chironomid assemblage. Diagram plotted on sediment depth (cm) with a secondary scale (cal. yr. BP) plotted for comparison. The sedimentological profile is plotted to the left of the curves.

Figure 6 Chironomid inferred July air temperature (CI-T) reconstructions from Lake Uddelermeer with sample specific error estimates. Curves plotted on age (cal. yr. BP) with a secondary scale of sediment depth (cm) plotted for comparison. Warm (red) and cold (blue) periods for the period 2550 - 1140 cal. yr. BP are indicated; the part of the record which is not included in the reconstruction is shown in grey. To the right of the reconstruction, the distance of the fossil sample to the nearest modern analogues in the Norwegian/Alpine training set (squared χ^2 -distance (sq. χ^2 d.): the vertical lines indicate the 2nd and 5th percentiles of all squared χ^2 -distances in the Norwegian/Alpine training set and are defined here as 'no close' and 'no good' analogues respectively (after Birks et al. 1990); the goodness-of-fit of the fossil samples to temperature (squared residual distance; sq.res.d): the vertical lines indicate the 90th and 95th percentiles in residual distances of the modern samples to the first axis in a constrained CCA and are defined here as a 'poor' and 'very poor' fit respectively (e.g. Birks et al. 1990); and the cumulative percentage

(Frequency %) of fossil chironomids that are absent (%absent) from the modern calibration set are given

Figure 7 CI-T reconstructions for Lake Uddelermeer (this paper); Bigland Tarn (Barber et al. 2013) and Talkin Tarn (Langdon et al. 2004) plotted on a cal. yr. BP timescale. Calibrated AMS radiocarbon dates and their 2 sigma error ranges are plotted to the right of each temperature reconstruction.

Figure 8 Warm (red) and cold (blue) periods in NW European temperature reconstructions for the period 1000 - 2500 cal. yr. BP (grey is not identified/available). IA: Iron Age; RWP: Roman Warm Period; DACP: Dark Age Cold Period; MCA: Medieval Climate Anomaly. A: CI-July air temperature Uddelermeer (this paper); B: CI-July air temperature Bigland tarn UK(Barber et al. 2013) also included in overview record D; C:Tree ring inferred JJA temperature for the Alps (Büntgen et al. 2011) also included in overview records D, E and F; D:Compilation various archives from NW Europe summer - winter and annual temperature (Riechelmann and Gouw-Bouman 2019); E:Compilation various archives N Hemisphere summer - winter - annual temperature (Ljungqvist 2009); F: compilation various archives globally temperature (Helama et al. 2017a). For the records A and C zone boundaries were placed where the temperature curve crossed the mean. When available, age uncertainty (minimum and maximum of the age model) is plotted with black lines.